

RESEARCH ARTICLE

# Trichostatin A attenuates ventilation-augmented epithelial-mesenchymal transition in mice with bleomycin-induced acute lung injury by suppressing the Akt pathway

Li-Fu Li<sup>1,2</sup>, Chung-Shu Lee<sup>1</sup>, Chang-Wei Lin<sup>1</sup>, Ning-Hung Chen<sup>1,2</sup>, Li-Pang Chuang<sup>1</sup>, Chen-Yiu Hung<sup>1</sup>, Yung-Yang Liu<sup>3,4\*</sup>

**1** Department of Internal Medicine, Division of Pulmonary and Critical Care Medicine, Chang Gung Memorial Hospital and Chang Gung University, Taoyuan, Taiwan, **2** Department of Respiratory Therapy, Chang Gung Memorial Hospital, Taoyuan, Taiwan, **3** Chest Department, Taipei Veterans General Hospital, Taipei, Taiwan, **4** Institutes of Clinical Medicine, School of Medicine, National Yang-Ming University, Taipei, Taiwan

\* [yyliau1103@gmail.com](mailto:yyliau1103@gmail.com)



**OPEN ACCESS**

**Citation:** Li L-F, Lee C-S, Lin C-W, Chen N-H, Chuang L-P, Hung C-Y, et al. (2017) Trichostatin A attenuates ventilation-augmented epithelial-mesenchymal transition in mice with bleomycin-induced acute lung injury by suppressing the Akt pathway. PLoS ONE 12(2): e0172571. doi:10.1371/journal.pone.0172571

**Editor:** Jung Weon Lee, Seoul National University College of Pharmacy, REPUBLIC OF KOREA

**Received:** December 1, 2016

**Accepted:** February 7, 2017

**Published:** February 24, 2017

**Copyright:** © 2017 Li et al. This is an open access article distributed under the terms of the [Creative Commons Attribution License](https://creativecommons.org/licenses/by/4.0/), which permits unrestricted use, distribution, and reproduction in any medium, provided the original author and source are credited.

**Data Availability Statement:** All relevant data are within the paper and its Supporting Information files.

**Funding:** This research was supported by the Ministry of Science and Technology (<https://www.most.gov.tw>) (105-2314-B-182A-091-MY2; to LFL) and Chang Gung Medical Research Project (<https://www.cgmh.org.tw>) (CMRPG3E1712; to CSL). The funders had no role in study design, data

## Abstract

### Background

Mechanical ventilation (MV) used in patients with acute respiratory distress syndrome (ARDS) can cause diffuse lung inflammation, an effect termed ventilator-induced lung injury, which may produce profound pulmonary fibrogenesis. Histone deacetylases (HDACs) and serine/threonine kinase/protein kinase B (Akt) are crucial in modulating the epithelial–mesenchymal transition (EMT) during the reparative phase of ARDS; however, the mechanisms regulating the interactions among MV, EMT, HDACs, and Akt remain unclear. We hypothesized that trichostatin A (TSA), a HDAC inhibitor, can reduce MV-augmented bleomycin-induced EMT by inhibiting the HDAC4 and Akt pathways.

### Methods

Five days after bleomycin treatment to mimic acute lung injury (ALI), wild-type or Akt-deficient C57BL/6 mice were exposed to low-tidal-volume (low- $V_T$ , 6 mL/kg) or high- $V_T$  (30 mL/kg) MV with room air for 5 h after receiving 2 mg/kg TSA. Nonventilated mice were examined as controls.

### Results

Following bleomycin exposure in wild-type mice, high- $V_T$  MV induced substantial increases in microvascular leaks; matrix metalloproteinase-9 (MMP-9) and plasminogen activator inhibitor-1 proteins; free radical production; Masson's trichrome staining; fibronectin, MMP-9, and collagen 1a1 gene expression; EMT (identified by increased localized staining of  $\alpha$ -smooth muscle actin and decreased staining of E-cadherin); total HDAC activity; and HDAC4 and Akt activation ( $P < 0.05$ ). In Akt-deficient mice, the MV-augmented lung inflammation, profibrotic mediators, EMT profiles, Akt activation, and pathological fibrotic scores were reduced and pharmacologic inhibition of HDAC4 expression was triggered by TSA ( $P < 0.05$ ).

collection and analysis, decision to publish, or preparation of the manuscript.

**Competing interests:** The authors declare that they have no competing interests.

**Abbreviations:** Akt, serine/threonine kinase/protein kinase B; ALI, acute lung injury; ARDS, acute respiratory distress syndrome; BAL, bronchoalveolar lavage; ECM, extracellular matrix; EBD, Evans blue dye; EMT, epithelial-mesenchymal transition; HDAC, histone deacetylases; IPF, idiopathic pulmonary fibrosis; MAPK, mitogen-activated protein kinase;  $\mu$ CT, micro-computer tomography; MMP-9, matrix metalloproteinase-9; MV, mechanical ventilation; PAI-1, plasminogen activator inhibitor-1; PCR, polymerase chain reaction;  $\alpha$ -SMA,  $\alpha$ -smooth muscle actin; TEM, transmission electron microscopy; TGF- $\beta$ 1, transforming growth factor- $\beta$ 1; TSA, trichostatin A; VILI, ventilator-induced lung injury;  $V_T$ , tidal volume.

## Conclusions

Our data indicate that TSA treatment attenuates high- $V_T$  MV-augmented EMT after bleomycin-induced ALI, in part by inhibiting the HDAC4 and Akt pathways.

## Introduction

Acute respiratory distress syndrome (ARDS) is characterized by a severe inflammatory reaction and epithelial injury followed by fibroblast proliferation and extracellular matrix (ECM) deposition, which requires mechanical ventilation (MV) to provide life support [1, 2]. High-tidal-volume (high- $V_T$ ) MV can initiate and propagate pulmonary neutrophil sequestration, enhanced alveolar–capillary membrane permeability, and the accumulation of protein-rich pulmonary edema; this ultimately leads to subsequent fibroproliferation and impaired gas exchange, a phenomenon termed ventilator-induced lung injury (VILI) [3, 4]. The epithelial–mesenchymal transition (EMT) process has been identified to mediate VILI-associated lung fibrosis by acquiring the phenotype of myofibroblasts differentiated from epithelial cells in both in vitro and in vivo studies [5–8]. Acute inflammation is followed by EMT, collagen deposition, and lung fibrosis through the production of profibrotic cytokines, including transforming growth factor (TGF)- $\beta$ , plasminogen activator inhibitor (PAI)-1, and matrix metalloproteinase (MMP)-9 [8, 9]. Patients with ARDS who developed progressive lung fibrosis exhibit poor clinical prognosis [1, 2, 10]; therefore, strategies to ameliorate the fibroproliferative activity may enhance survival and improve quality of life.

Acetylation is one of the most crucial posttranslational modifications of histones that determines the structure and function of chromatin, and is hence related to gene transcription [11, 12]. Histone deacetylases (HDACs) are crucial posttranslational modifiers that remove acetyl groups from histones and transcription factors, and epigenetically regulate the expression of various genes [11, 12]. HDACs have been proven to be involved in fibrogenesis in various organs, including the lungs [13–17]. For example, Korfei et al. identified aberrant overexpression and activity of HDACs in the lungs of patients with idiopathic pulmonary fibrosis (IPF) [15]. Notably, HDAC4 is necessary for the TGF- $\beta$ -induced fibroblast to myofibroblast transition because it inhibits histone acetylation [18, 19]. Furthermore, HDAC4 knockdown was reported to inhibit TGF- $\beta$  signaling, indicating the essential role of HDAC4 in the epigenetic regulation of myofibroblast transdifferentiation in human lung fibroblasts [19].

Following acute inflammation, excessive reactive oxygen species (ROS) can induce damaged pulmonary epithelia to secrete proinflammatory and profibrotic cytokines that lead to imbalances between histone acetylation and deacetylation [20]. In rodents, PAI-1 and MMP-9 were shown to be essential cytokines for the recruitment of neutrophils (a primary source of ROS in acute lung injury [ALI]) and subsequent ECM remodeling in VILI pathogenesis [1, 9, 21]. However, the molecular mechanisms of HDACs, inflammatory-cytokines, and VILI-associated lung fibrosis remain unclear. HDAC inhibitors can act as effective anti-inflammatory or antifibrotic drugs by changing histone acetylation or suppressing the transcription factors [22–26]. Trichostatin A (TSA), a hydroxamic acid, has been identified as the histone deacetylase inhibitor with the most potential among all class I and class II HDACs [1]. Several in vitro studies have demonstrated that TSA can attenuate EMT by restoring epithelial cadherin expression in renal tubular epithelial cells, hepatocytes, lens epithelial cells, and airway epithelial cells [14, 17, 27, 28]. TSA has also been identified to suppress  $\alpha$ -smooth muscle actin ( $\alpha$ -SMA) expression and collagen production in rat hepatic stellate cells, rat skin fibroblasts, and

primary human skin fibroblasts [29–31]. Furthermore, the prevention of ECM deposition and fibrotic scores has been achieved using TSA in the mouse models of bleomycin-induced skin fibrosis and pulmonary fibrosis, respectively [32, 33].

The activation of Akt is critical in mediating the differentiation of mesenchymal cells into smooth muscle cells [34]. A previous *in vitro* study demonstrated that Akt phosphorylation was modulated by HDAC4 in the regulation of TGF- $\beta$ 1-mediated  $\alpha$ -SMA expression [19]. Additionally, Tan et al. showed that Akt plays a role in regulating bleomycin-induced EMT in mice [35]. In our previous study, we demonstrated that high- $V_T$  ventilation-aggravated pulmonary fibrosis was dependent on the activation of the Akt pathway using an *in vivo* bleomycin mouse model [36]. However, the relationships between the Akt pathway and mechanical stretch-induced epigenetic programming remain unclear. In the present high- $V_T$  MV-induced lung fibrosis model in mice pretreated with bleomycin, we first explored whether TSA could inhibit MV-augmented bleomycin-induced EMT and pulmonary fibrosis. Subsequently, we compared the effects of various tidal volumes of MV and examined the role of Akt kinase in the anti-inflammatory and antifibrotic effects of TSA on Akt-deficient mice. We hypothesized that following bleomycin-induced ALI, TSA administration can ameliorate high- $V_T$  mechanical stretch-augmented EMT by suppressing the HDAC4 and Akt pathways.

## Materials and methods

### Ethics of experimental animals

Wild-type or Akt-deficient C57BL/6 mice, aged between 6 and 8 weeks, weighing between 20 and 25 g, were obtained from Jackson Laboratories (Bar Harbor, ME) and National Laboratory Animal Center (Taipei, Taiwan), as described in our previous study [36]. We performed the experiments in accordance with the National Institutes of Health Guidelines on the Use of Laboratory Animals. The Institutional Animal Care and Use Committee of Chang Gung Memorial Hospital approved the protocol (Permit number: 2015101201).

### Experimental groups

Animals were randomly distributed into 6 groups in each experiment: group 1, control, non-ventilated wild-type mice without bleomycin; group 2, control, nonventilated wild-type mice with bleomycin; group 3,  $V_T$  6 mL/kg wild-type mice with bleomycin; group 4,  $V_T$  30 mL/kg wild-type mice with bleomycin; group 5,  $V_T$  30 mL/kg Akt<sup>+/-</sup> mice with bleomycin; group 6,  $V_T$  30 mL/kg wild-type mice with bleomycin and 2 mg/kg TSA administration. In each group, three mice underwent micro-computed tomography (micro-CT) and five mice underwent measurement for Evans blue dye (EBD) assay, lung edema, bronchoalveolar lavage (BAL) fluid total protein, malondialdehyde, PAI-1 and MMP-9 production, Masson's trichrome stain, total collagen and hydroxyproline contents, collagen gene expression, immunofluorescence labeling, fibrosis scoring, Western blot, and immunohistochemistry assay.

### Ventilator protocol

We used our established mouse model of VILI, as previously described [8]. In brief, a 20-gauge angiocatheter was introduced into the tracheotomy orifice of mice and general anesthesia was maintained by regular intraperitoneal administration of zoletil 50 (5 mg/kg) and xylazine (5 mg/kg) at the beginning of experiment and every 30 min. Five hours of MV was applied for western blot, real-time polymerase chain reaction (PCR), PAI-1 and MMP-9 production, lung water, EBD, total collagen, collagen gene, free radicals, histologic staining analyses, and micro-CT imaging, based on our time course and previous studies [8, 36]. At the end of the study

period, heparinized blood was taken from the arterial line for analysis of arterial blood gas, and the mice were sacrificed by exsanguination under zoletil and xylazine anesthesia to minimize suffering. The nonventilated control mice were anesthetized and sacrificed immediately.

### Bleomycin and trichostatin A administration

HDAC inhibitor (trichostatin A, Sigma, St. Louis, MO) 2 mg/kg was given intraperitoneally 1 h before ventilation based on our present and previous studies that showed 2 mg/kg inhibited HDAC activity [19]. The mice received a single dosage of 0.075 units of bleomycin in 100  $\mu$ L of sterile normal saline solution intratracheally (Sigma, St. Louis, MO) and were ventilated 5 days after the administration of bleomycin [8].

### Immunofluorescence labeling

The lung tissues were paraffin embedded, sliced at 4  $\mu$ m, deparaffinized, and stained according to the manufacturer's instruction for an immunohistochemical kit (Santa Cruz Biotechnology, Santa Cruz, CA). Lung sections were incubated with primary rabbit anti-mouse antibodies of E-cad and  $\alpha$ -SMA (1:100; New England BioLabs, Beverly, MA) and fluorescent secondary antibodies of FITC-conjugated affinity purified anti-goat (E-cad) and Cy3-conjugated anti-rabbit (E-cad and  $\alpha$ -SMA) (1:1000; Santa Cruz Biotechnology, Santa Cruz, CA). Nuclear staining was performed using Hoechst solution (0.5  $\mu$ g/mL; Sigma, St. Louis, MO). The fluorescence-labeled slides were subsequently examined using a Leica TCS 4D confocal laser scanning microscopy system (Leica, Wetzlar, Germany).

### Extraction of nuclear protein

The lungs (0.12–0.17 g) were homogenized in buffer A (lysis buffer) containing 50 mM KCl, 0.5% Igepal CA-630, 25 mM HEPES (pH 7.8), 1 mM PMSF, 2  $\mu$ M leupeptin, 20  $\mu$ g/mL aprotinin, 100  $\mu$ M DTT and were subsequently incubated 5 min on ice, as previously described [37]. Cells were collected by centrifugation at 310 g, and the supernatant was decanted. The nuclei were washed in buffer A without Igepal CA-630, collected at 310 g, and resuspended in buffer B (extraction buffer) containing 500 mM KCl, 25 mM HEPES (pH 7.8), 10% glycerol, 1 mM PMSF, 2  $\mu$ M leupeptin, 20  $\mu$ g/mL aprotinin, and 100  $\mu$ M DTT for 5 min on ice. The samples were subsequently frozen and thawed twice by dry ice and a 37°C water bath, rotating 20 min at 4°C, and centrifuged at 15,350 g for 20 min. The clear supernatant was collected, and nuclear protein concentration was measured by the Bradford method.

### Immunoblot analysis

The lungs were homogenized in 3 mL of lysis buffer (20 mM HEPES pH 7.4, 1% Triton X-100, 10% glycerol, 2 mM ethylene glycol-bis ( $\beta$ -aminoethyl ether)-N, N, N', N'-tetraacetic acid, 50  $\mu$ M  $\beta$ -glycerophosphate, 1 mM sodium orthovanadate, 1 mM dithiothreitol, 400  $\mu$ M aprotinin, and 400  $\mu$ M phenylmethylsulfonyl fluoride), transferred to eppendorf tubes and placed on ice for 15 min. Tubes were centrifuged at 15,350 g for 10 min at 4°C and supernatant was flash frozen. Crude cell lysates (Akt) and nuclear protein (HDAC 2 and HDAC4) were matched for protein concentration, resolved on a 10% bis-acrylamide gel, and electrotransferred to Immobilon-P membranes (Millipore Corp., Bedford, MA). For assay of Akt phosphorylation, and Akt, GAPDH, HDAC2, and HDAC4 total protein expression, Western blot analysis was performed with antibodies of phospho-Akt, Akt, GAPDH, HDAC2, and HDAC4 (New England BioLabs, Beverly, MA). Blots were developed by enhanced chemiluminescence (NEN Life Science Products, Boston, MA).

## Immunohistochemistry

The lungs were paraffin embedded, sliced at 4  $\mu\text{m}$ , deparaffinized, antigen unmasked in 10 mM sodium citrate (pH 6.0), incubated with phospho-Akt primary antibody (1:100; New England BioLabs, Beverly, MA), and biotinylated goat anti-rabbit secondary antibody (1:100) according to the manufacturer's instruction for an immunohistochemical kit (Santa Cruz Biotechnology, Santa Cruz, CA). The specimens were further conjugated with horseradish peroxidase-streptoavidin complex, detected with a diaminobenzidine (DAB) substrate mixture, and counterstained by hematoxylin. A dark-brown DAB signal, identified by arrows, indicated positive staining of phospho-Akt of epithelial cells, whereas shades of light blue signified non-reactive cells.

## Measurement of MMP-9 and PAI-1

At the end of the study period, the lungs were lavaged via tracheostomy with 20-gauge angiocatheter (sham instillation) 3 times with 0.6 mL of 0.9% normal saline. The effluents were pooled and centrifuged at 310  $g$  for 10 min. Supernatants were frozen at  $-80^{\circ}\text{C}$  for further analysis of the cytokines. MMP-9 and PAI-1 with lower detection limit of 0.014 ng/mL and 0.02 ng/mL were measured in BAL fluid by using commercially available immunoassay kits containing primary polyclonal anti-mouse antibody that was cross-reactive with rat and mouse MMP-9 and PAI-1 (MMP-9: Biosource International, Camarillo, CA; PAI-1: Molecular Innovations Inc., Southfield, MI). Each sample was run in duplicate according to the manufacturer's instructions.

## Total HDAC activity assay

The nuclear protein extracted from lung tissue was incubated with assay buffer and *Color de Lys* substrate using a HDAC colorimetric assay/drug discovery kit (Enzo Life Sciences International, Inc., Plymouth Meeting, PA) and read on a standard microplate reader at 405 nm. Total HDAC activity was expressed relative to standard curve generated from 0–500  $\mu\text{M}$  *Color de Lys* deacetylated standard.

## Real-time polymerase chain reaction

For isolating total RNA, the lung tissues were homogenized in TRIzol reagents (Invitrogen Corporation, Carlsbad, CA) according to the manufacturer's instructions. Total RNA (1  $\mu\text{g}$ ) was reverse transcribed by using a GeneAmp PCR system 9600 (PerkinElmer, Life Sciences, Inc., Boston, MA), as previously described [8]. The following primers were used for real-time polymerase chain reaction (PCR): HDAC 4, forward primer 5'– CTGGCATCCCTGTGTCAT TTG –3' and reverse primer 5'– ACACAAGACCTGTGGTGAAC CTT –3'; and GAPDH as internal control, forward primer 5'– AATGCATCCTGCACCACCA A –3' and reverse primer 5'– gtagccatattcattgtcata –3' (Integrated DNA Technologies, Inc., Coralville, IA)[38]. All quantity PCR reactions using SYBR Master Mix were performed on an ABI Prism 7000 sequence detector PCR system (Applied Biosystems, Foster City, CA).

## Statistical evaluation

The Western blots were quantitated using a National Institutes of Health (NIH) image analyzer Image J 1.27z (National Institutes of Health, Bethesda, MD) and presented as arbitrary units. Values were expressed as the mean  $\pm$  SD from at least 5 separate experiments. The data of EBD analysis, lung wet-to-dry weight ratio, BAL total protein, MDA, MMP-9, PAI-1, total collagen content, collagen gene expression, fibrosis score, and histopathologic assay were

analyzed using Statview 5.0 (Abascus Concepts Inc. Cary, NC; SAS Institute, Inc.). All results of Western blots and real-time PCR were normalized to the nonventilated control wild-type mice with bleomycin treatment. ANOVA was used to assess the statistical significance of the differences, followed by multiple comparisons with a Scheffe's test, and a P value < 0.05 was considered statistically significant. BAL total protein, collagen assay, collagen gene 1a expression, EBD analysis, histopathological grading of VILI, MDA, analysis of lung water, Masson's trichrome stain, fibrosis scoring, and micro-CT were performed as previously described [8, 36].

## Results

### Reduction of VILI by TSA

High- $V_T$  (30 mL/kg) and low- $V_T$  (6 mL/kg) MV with room air was applied for 5 h to induce VILI in mice and elucidate the injurious effects of overstretch and treatment effects of intraperitoneally delivered TSA. The physiological conditions at the beginning and end of ventilation are listed in Table 1. The normovolemic statuses of the mice were maintained by monitoring their mean artery pressure. Additionally, the lung EBD microvascular leak, wet-to-dry weight ratio, and BAL fluid total protein were measured to determine the effects of high- $V_T$  ventilation on microvascular leaks and lung edemas in VILI (Fig 1A–1C). Furthermore, the oxidant load and inflammatory cytokine levels were measured to determine the level of oxidative stress and amount of profibrogenic cytokines for fibroblasts in VILI (Fig 1D–1F). A higher wet-to-dry weight ratio and elevated levels of EBD, BAL fluid total protein, malondialdehyde (an aldehydic secondary product of lipid peroxidation), MMP-9, and PAI-1

**Table 1. Physiologic conditions at the beginning and end of ventilation.**

	Control without bleomycin wild-type	Control with bleomycin wild-type	$V_T$ 6 mL/kg with bleomycin wild-type	$V_T$ 30 mL/kg with bleomycin wild-type	$V_T$ 30 mL/kg with bleomycin Akt <sup>+/−</sup>	$V_T$ 30 mL/kg with bleomycin wild-type, TSA
PH	7.42±0.04	7.38±0.03	7.36±0.05	7.35±0.06	7.36±0.05	7.37±0.08
PaO <sub>2</sub> (mmHg)	97.9±0.4	96.1±0.1	85.4±0.7*	76.5±1.4*†	86.9±1.2*	83.9±1.3*
A-aDO <sub>2</sub> (mmHg)	3.3±0.2	4.6±0.1	13.1±0.2*	27.6±0.5*†	17.0±0.4*	19.9±0.5*
PaCO <sub>2</sub> (mmHg)	39.1±0.3	39.4±0.2	41.2±0.3	36.7±0.8	36.8±1.4	36.9±1.8
MAP (mmHg)						
Start	85±0.8	83±0.6	83.4±1.2	82.4±1.5	83.2±1.5	82.7±1.6
End	83±0.7	81±0.4	79.6±1.5	73.7±4.4*†	78.8±1.9*	76.52±4.1*
PIP, mm Hg						
Start			9.8±1.1	23.7±1.4	23.4±1.9	23.5±1.0
End			11.9±0.8	28.5±2.1	26.8±1.7	27.4±2.5

At the end of the study period, arterial blood gases and mean arterial pressure were obtained from the nonventilated control mice and mice subjected to tidal volume at 6 mL/kg or at 30 mL/kg for 5 h (n = 10 per group). The normovolemic statuses of mice were maintained by monitoring mean artery pressure. Data are presented as mean ± SD. ANOVA was used to assess the statistical significance of the differences, followed by multiple comparisons with a Scheffe's test, and a P value < 0.05 was considered statistically significant.

\* P < 0.05 versus the nonventilated control mice with bleomycin pretreatment.

† P < 0.05 versus all other groups.

A-aDO<sub>2</sub> = alveolar-arterial oxygen gradient; Akt<sup>+/−</sup> = serine/threonine kinase/protein kinase B-deficient mice; MAP = mean arterial pressure; PIP = peak inspiratory pressure; TSA = trichostatin A;  $V_T$  = tidal volume. The physiological data of the control groups were similar during the experiment and were used as the beginning data of ventilation.

doi:10.1371/journal.pone.0172571.t001

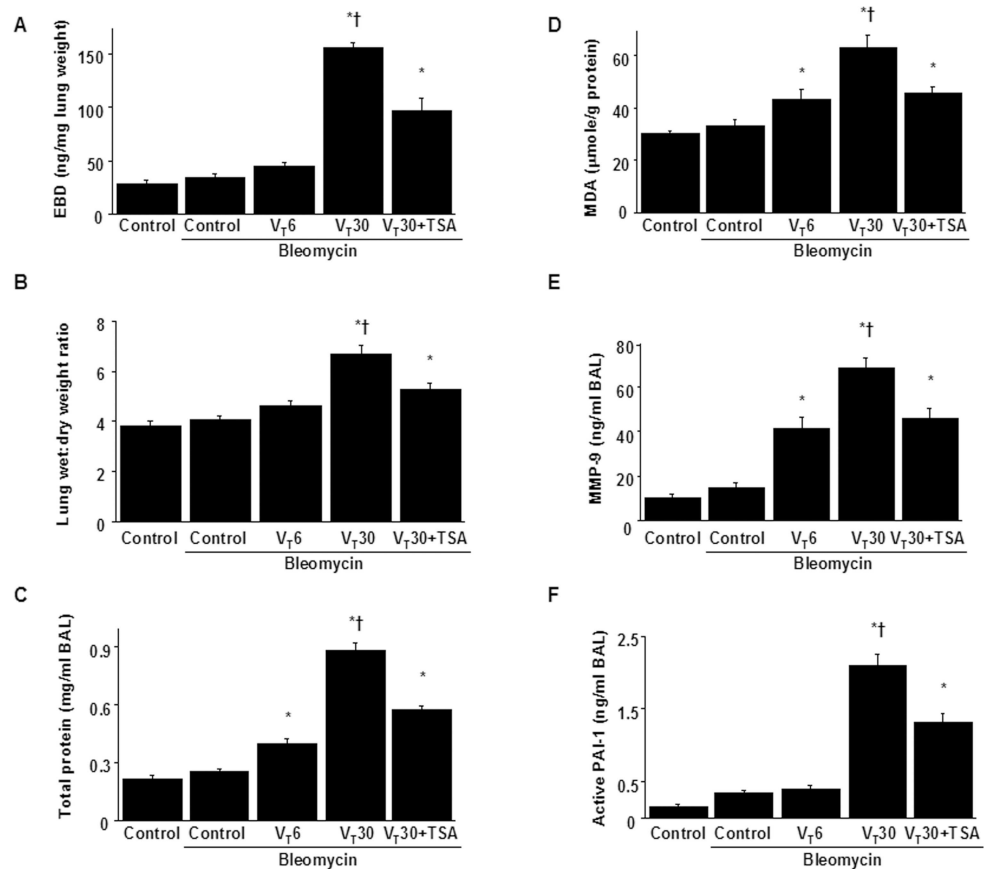


**Fig 1. Trichostatin A inhibited lung stretch-induced microvascular leak, lung edema, oxygen radicals, MMP-9 and PAI-1 production.** Five days after administering bleomycin, Evans blue dye analysis (A), lung wet-to-dry-weight ratio (B), BAL fluid total protein (C), MDA (D), MMP-9 (E) and PAI-1 (F) secretion in BAL fluid (E) were from the lungs of nonventilated control mice and mice ventilated at a tidal volume of 6 mL/kg (V<sub>T</sub> 6) or 30 mL/kg (V<sub>T</sub> 30) for 5 h with room air (n = 5 per group). TSA 2 mg/kg was given intraperitoneally 1 h before mechanical ventilation. ANOVA was used to assess the statistical significance of the differences, followed by multiple comparisons with a Scheffe's test, and a P value < 0.05 was considered statistically significant. \* P < 0.05 versus the nonventilated control mice with bleomycin pretreatment; †P < 0.05 versus all other groups. BAL = bronchoalveolar lavage; EBD = Evans blue dye; MDA = malondialdehyde; MMP-9 = matrix metalloproteinase-9; PAI-1 = plasminogen activator inhibitor-1; TSA = trichostatin A.

doi:10.1371/journal.pone.0172571.g001

protein were observed in the mice subjected to a V<sub>T</sub> of 30 mL/kg compared with those subjected to a V<sub>T</sub> of 6 mL/kg and the nonventilated control mice. Overall, TSA administration substantially suppressed the high-V<sub>T</sub> MV-induced increase in lung inflammation.

### Suppression of MV-induced HDAC4 activation by TSA

Because HDAC activation has been reported to play a crucial role in regulating stretch-induced EMT [18, 19, 28], we measured HDAC expression to investigate the role of HDAC signaling in our VILI model (Fig 2). The total HDAC activity, HDAC4 expression, and HDAC4 mRNA expression were increased in the mice subjected to a V<sub>T</sub> of 30 mL/kg compared with those subjected to a V<sub>T</sub> of 6 mL/kg and the nonventilated control mice. Notably, HDAC2 expression did not change significantly after MV. Moreover, the elevation of stretch-induced HDAC4 activity was considerably attenuated by TSA through pharmacologic inhibition.

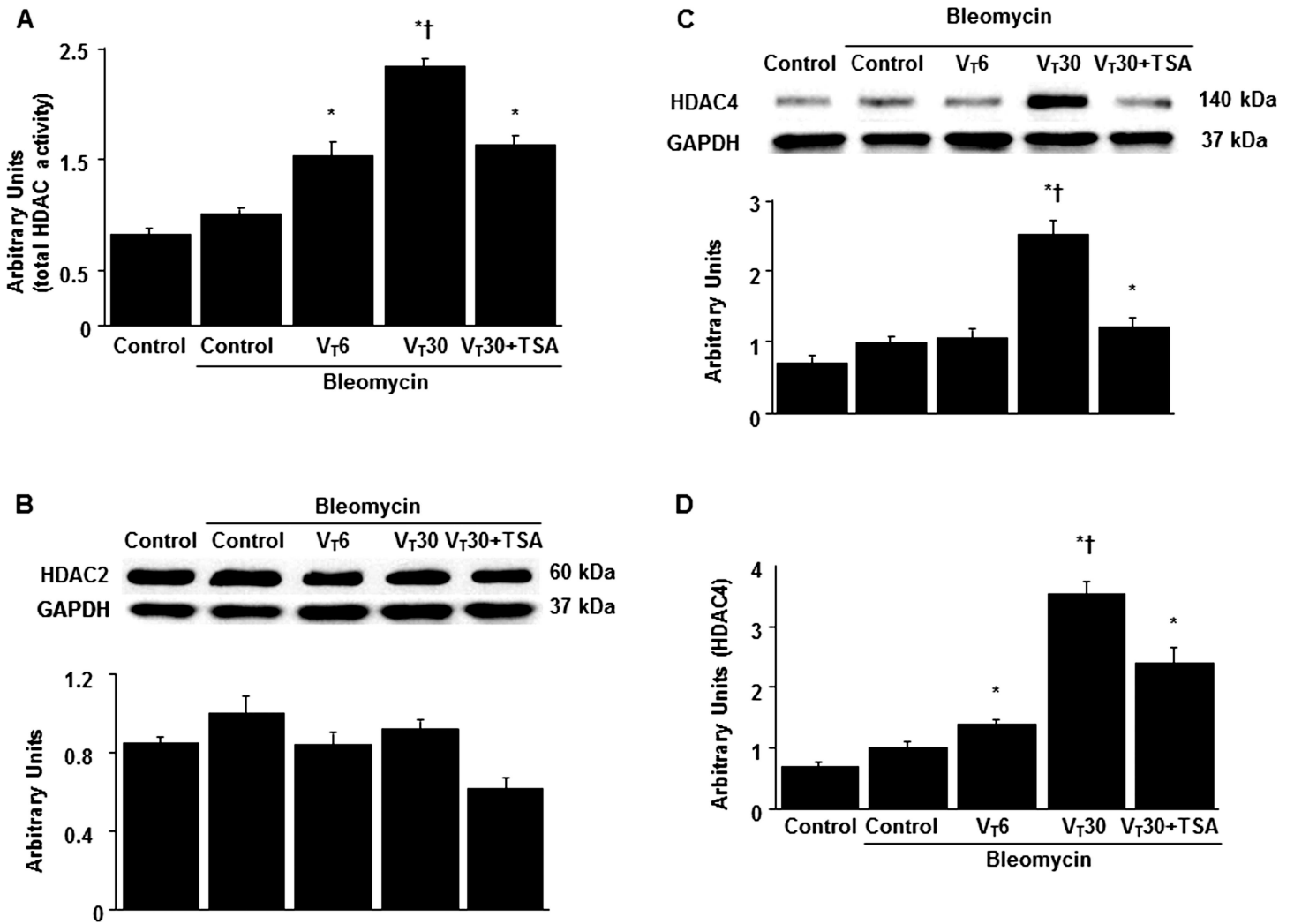


**Fig 2. Trichostatin A reduced lung stretch-induced activation of HDAC4.** (A) Five days after bleomycin treatment, total HDAC activity was from the lungs of nonventilated control mice and mice ventilated at a tidal volume of 6 mL/kg or 30 mL/kg for 5 h with room air (n = 5 per group). (B and C) Western blots performed using antibodies that recognize HDAC2, HDAC4, and GAPDH expression in lung tissue five days after bleomycin treatment were from nonventilated control mice and mice ventilated at a tidal volume of 6 mL/kg or 30 mL/kg for 5 h with room air (n = 5 per group). (D) Real-time polymerase chain reaction of HDAC4 mRNA and GAPDH mRNA expression in lung tissue after five days of bleomycin treatment were from nonventilated control mice and mice ventilated at a tidal volume of 6 mL/kg or 30 mL/kg for 5 h with room air (n = 5 per group). Arbitrary units were expressed as the ratio of HDAC2 to GAPDH, HDAC4 to GAPDH, and HDAC4 mRNA to GAPDH (n = 5 per group). TSA 2 mg/kg was given intraperitoneally 1 h before mechanical ventilation. ANOVA was used to assess the statistical significance of the differences, followed by multiple comparisons with a Scheffe's test, and a P value < 0.05 was considered statistically significant. \* P < 0.05 versus the nonventilated control mice with bleomycin pretreatment; † P < 0.05 versus all other groups. HDAC = histone deacetylase; GAPDH = glyceraldehyde-phosphate dehydrogenase.

doi:10.1371/journal.pone.0172571.g002

### Reduction of collagen fiber production and collagen gene expression in mice ECM by TSA

We also applied Masson's trichrome staining to assess the effects of MV on the accumulated peribronchiolar and parenchymal collagen fibers. We observed increased collagen fibers in the ECM in the mice subjected to a V<sub>T</sub> of 30 mL/kg compared with those subjected to a V<sub>T</sub> of 6 mL/kg and the nonventilated control mice (Fig 3A). Measured quantitatively according to total lung collagen and hydroxyproline content, the increase in collagen fibers was substantially diminished through pharmacologic inhibition by TSA (Fig 3B and 3C). In addition, we

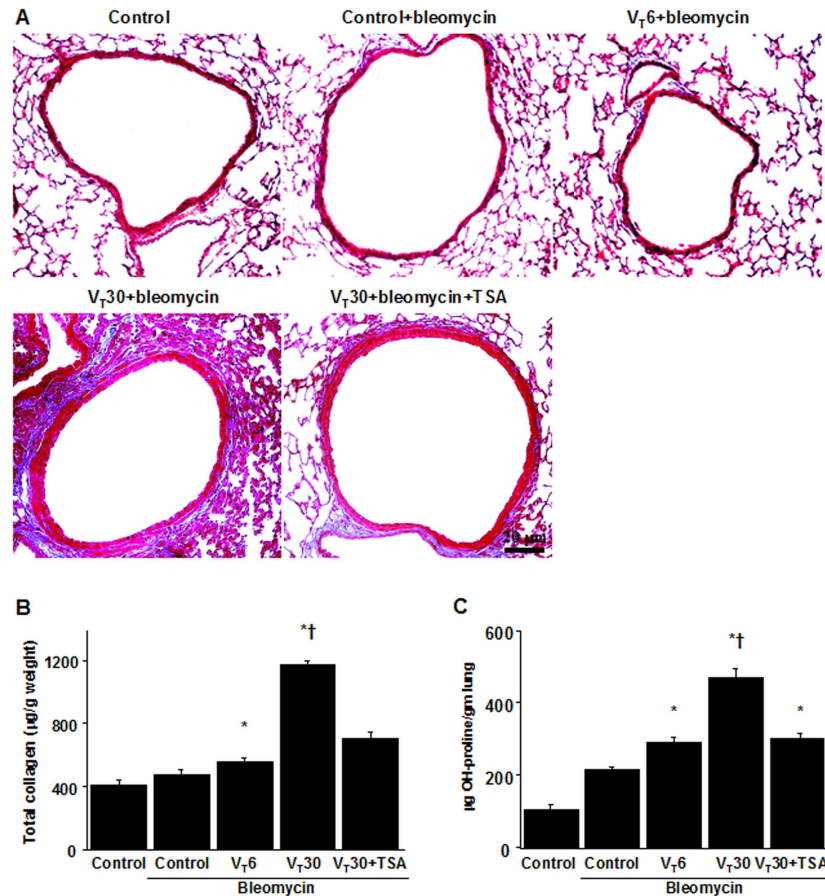


**Fig 3. Trichostatin A reduced lung stretch-induced collagen production.** Representative micrographs (x200) with Masson's trichrome staining of paraffin lung sections (A), total collagen (B), and hydroxyproline (OH) (C) of lung tissue after five days of bleomycin administration were from nonventilated control mice and mice ventilated at a tidal volume of 6 mL/kg or 30 mL/kg for 5 h with room air (n = 5 per group). TSA 2 mg/kg was given intraperitoneally 1 h before mechanical ventilation. Scale bars represent 20 µm. ANOVA was used to assess the statistical significance of the differences, followed by multiple comparisons with a Scheffe's test, and a P value < 0.05 was considered statistically significant. \* P < 0.05 versus the nonventilated control mice with bleomycin pretreatment; † P < 0.05 versus all other groups.

doi:10.1371/journal.pone.0172571.g003

used a real-time polymerase chain reaction to measure the expression of inflammation-associated collagens 1a1; fibronectin; and MMP-9. The expression of collagen 1a1, fibronectin, and MMP-9 was higher in the mice subjected to a V<sub>T</sub> of 30 mL/kg compared with those subjected to a V<sub>T</sub> of 6 mL/kg and the nonventilated control mice (Fig 4). Moreover, TSA administration appreciably reduced the expression of collagen 1a1, fibronectin, and MMP-9 associated with VILI.

### Inhibition of MV-induced fibrogenic markers by TSA

We detected the expression of E-cadherin (an epithelial marker) and α-SMA (a mesenchymal marker) through immunofluorescent staining, which revealed the cell types involved in the MV-induced EMT (Fig 5A). Moreover, we examined the effects of TSA administration in attenuating EMT. Overall, the mice subjected to a V<sub>T</sub> of 30 mL/kg experienced downregulation of E-cadherin and upregulation of α-SMA in their bronchiolar epithelia and peribronchiolar lung parenchymas, indicating a phenotype transition from epithelial cells to myofibroblasts. TSA also further increased the expression of E-cadherin and reduced the expression of α-SMA. In

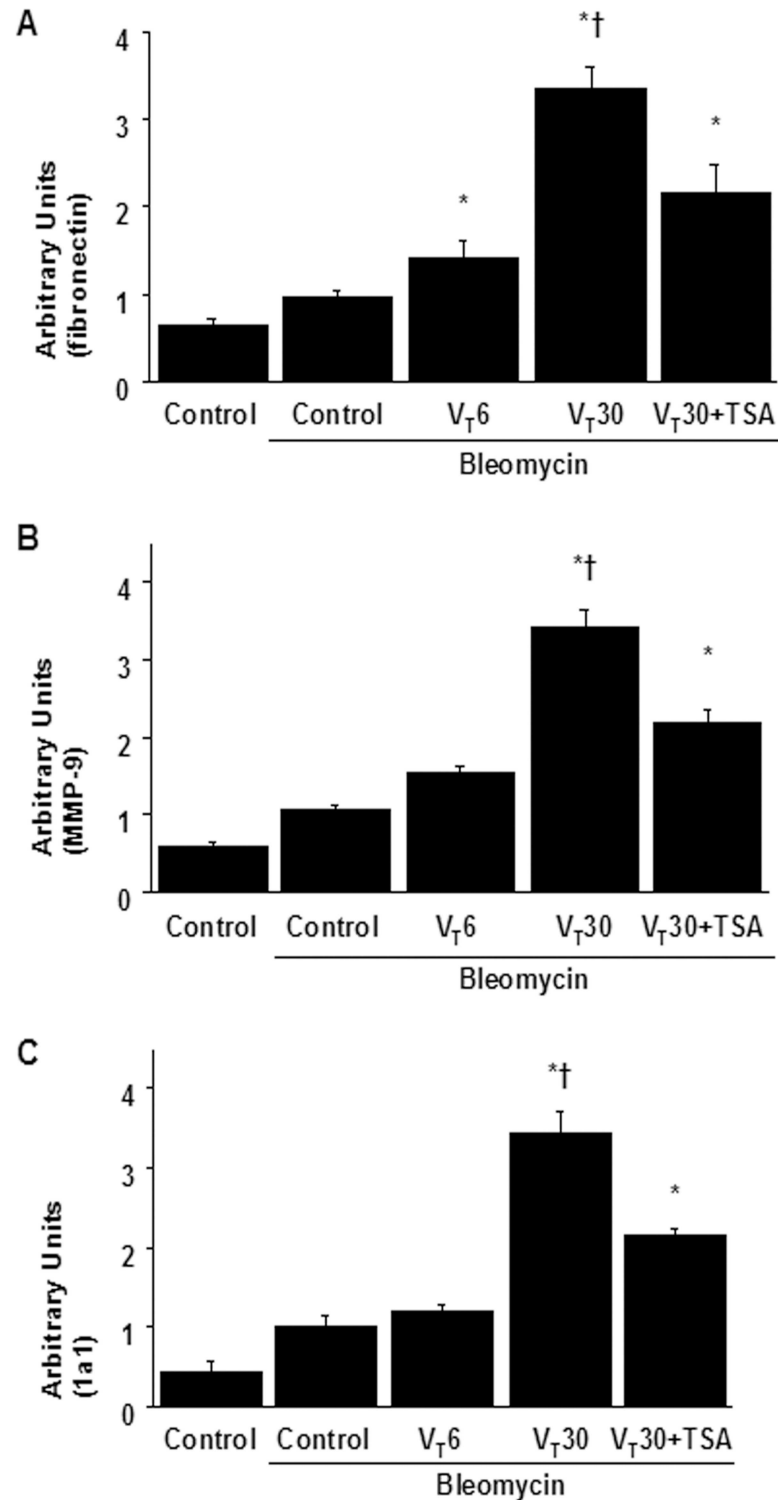


**Fig 4. Trichostatin A suppressed lung stretch-induced collagen gene expression.** After five days of bleomycin treatment, real-time polymerase chain reaction of fibronectin (A), MMP-9 (B), and 1a1 (C) mRNA expression were from the lungs of nonventilated control mice and mice ventilated at a tidal volume of 6 mL/kg or 30 mL/kg for 5 h with room air (n = 5 per group). Arbitrary units were expressed as the ratio of fibronectin, MMP-9, and 1a1 mRNA to GAPDH (n = 5 per group). TSA 2 mg/kg was given intraperitoneally 1 h before mechanical ventilation. ANOVA was used to assess the statistical significance of the differences, followed by multiple comparisons with a Scheffe's test, and a P value < 0.05 was considered statistically significant. \* P < 0.05 versus the nonventilated control mice with bleomycin pretreatment; † P < 0.05 versus all other groups.

doi:10.1371/journal.pone.0172571.g004

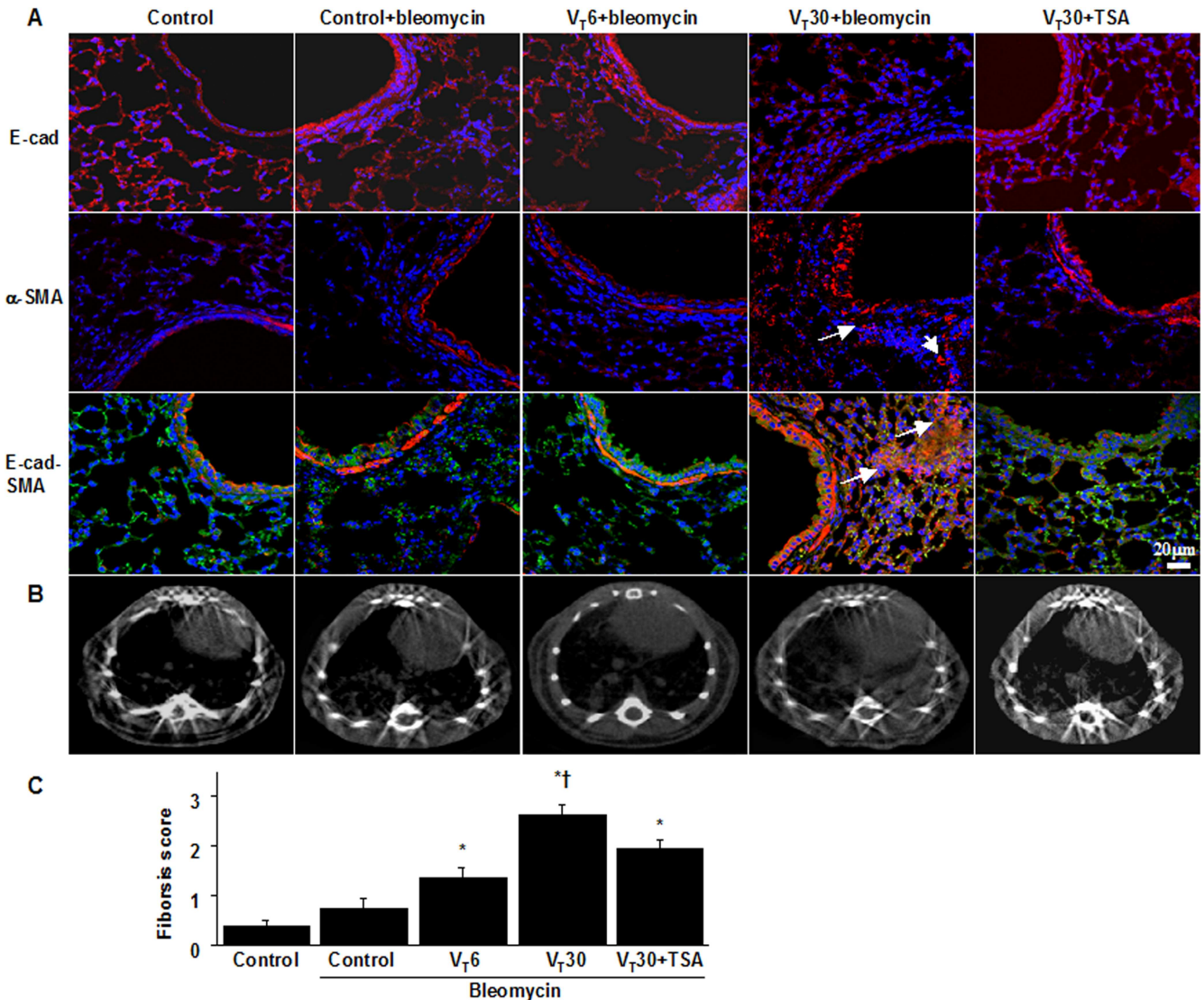


**Fig 5. Trichostatin A attenuated lung stretch-induced fibrogenic biomarkers.** Five days after bleomycin treatment, representative photomicrographs (x400) with E-cadherin (E-cad, red or bright green),  $\alpha$ -smooth muscle actin ( $\alpha$ -SMA, red), and Hoechst (blue) immunofluorescent staining of paraffin lung sections (A) ( $n = 5$  per group), and micro-computed tomography imaging (B) ( $n = 3$  per group) were from nonventilated control mice and mice ventilated at a tidal volume of 6 mL/kg or 30 mL/kg for 5 h with room air. TSA 2 mg/kg was given intraperitoneally 1 h before mechanical ventilation. Positive red and bright green staining in the lung epithelium and interstitium is identified by arrows ( $n = 5$  per group). The fibrotic scoring (C) was quantified as the average number of 10 nonoverlapping fields in Masson's trichrome staining of paraffin lung sections ( $n = 5$  per group). Scale bars represent 20  $\mu$ m. ANOVA was used to assess the statistical significance of the differences, followed by multiple comparisons with a Scheffe's test, and a P value < 0.05 was considered statistically significant. \* P < 0.05 versus the nonventilated control mice with bleomycin pretreatment; † P < 0.05 versus all other groups.

doi:10.1371/journal.pone.0172571.g005

addition, we employed micro-CT, a primary imaging technique that monitors lung fibrogenesis in vivo, to examine the damaged lung structure [39]. Evidence of pulmonary fibrogenesis and damage, including increased reticular opacities, honeycombing, traction bronchiectasis, and ground glass opacities in the lower lungs, was aggravated in the mice ventilated at a  $V_T$  of 30 mL/kg compared with those subjected to a  $V_T$  of 6 mL/kg and the nonventilated control mice (Fig 5B). To further determine the effects of MV on ECM deposition, we performed fibrosis scoring through Masson's trichrome staining (Figs 3A and 5C). Peribronchiolar ECM accumulation was elevated in the mice subjected to a  $V_T$  of 30 mL/kg compared with those subjected to

a  $V_T$  of 6 mL/kg and the nonventilated control mice. Additionally, TSA administration substantially reduced the fibrosis score of ventilation-induced lung fibrogenesis.

### Suppression of the MV-induced Akt pathway by TSA and Akt heterozygous knockout

Because Akt activation has been reported to regulate stretch-induced EMT [36, 40], we measured Akt phosphorylation to examine the role of the Akt pathway in our VILI model (Fig 6). The positive immunohistochemical staining for Akt in the airway epithelial cells of the mice

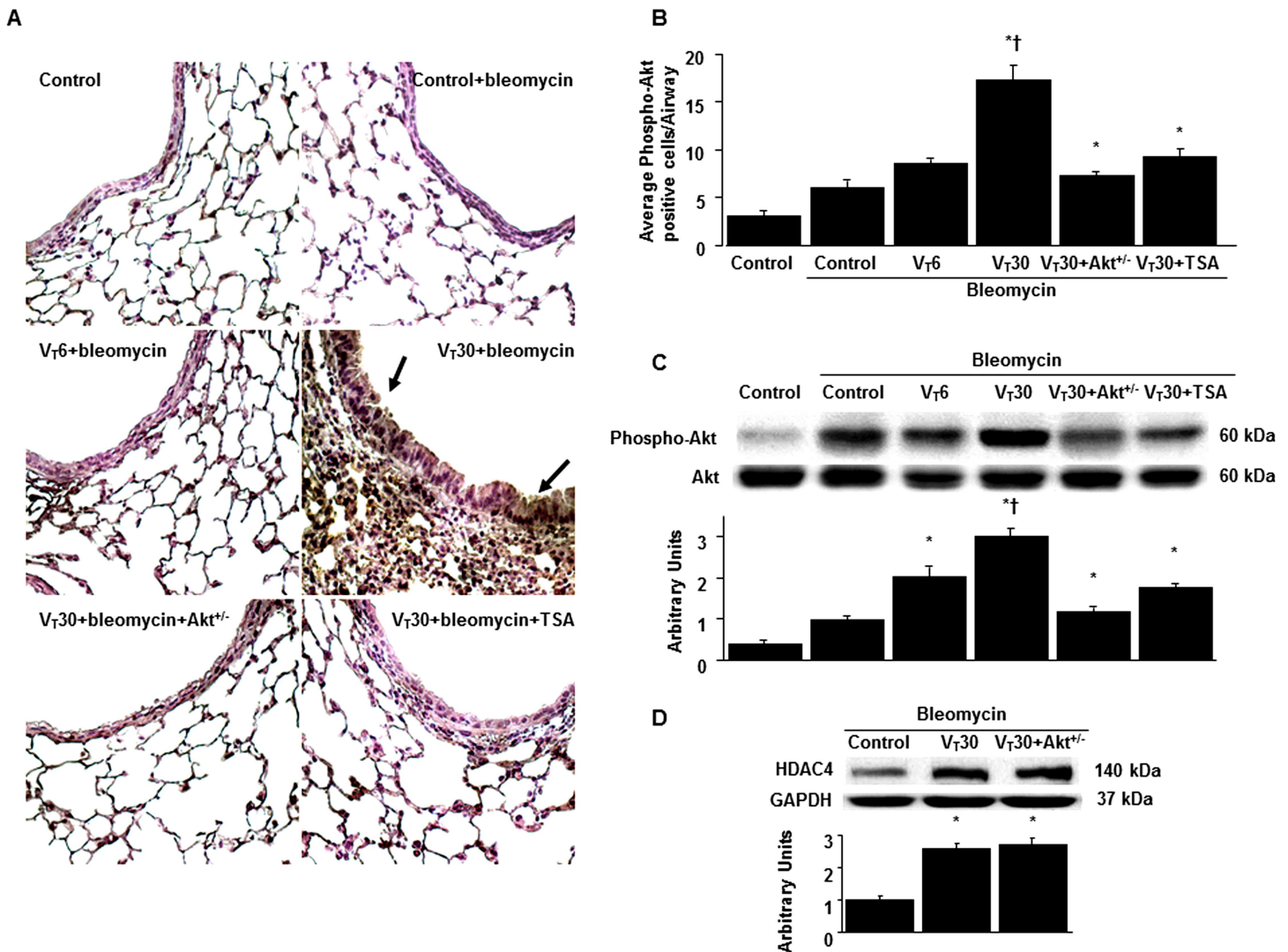


**Fig 6. Trichostatin A and Akt heterozygous knockout abrogated lung stretch-induced Akt phosphorylation.** (A and B) Representative micrographs (x400) with phosphorylated Akt staining of paraffin lung sections and quantification 5 days after administering bleomycin were from nonventilated control mice and mice ventilated at a tidal volume of 6 mL/kg or 30 mL/kg for 5 h with room air (n = 5 per group). (C and D) Western blots were performed using an antibody that recognizes the phosphorylated Akt expression and antibodies that recognize total Akt, HDAC4, and GAPDH expression in lung tissue five days after bleomycin treatment from nonventilated control mice and mice ventilated at a tidal volume of 6 mL/kg or 30 mL/kg for 5 h with room air (n = 5 per group). Arbitrary units were expressed as the ratio of phospho-Akt to Akt and HDAC4 to GAPDH (n = 5 per group). TSA 2 mg/kg was given intraperitoneally 1 h before mechanical ventilation. ANOVA was used to assess the statistical significance of the differences, followed by multiple comparisons with a Scheffe's test, and a P value < 0.05 was considered statistically significant. \* P < 0.05 versus the nonventilated control mice with bleomycin pretreatment; † P < 0.05 versus all other groups. Akt<sup>+/-</sup> = serine/threonine kinase-protein kinase (Akt)-deficient mice.

doi:10.1371/journal.pone.0172571.g006

subjected to a  $V_T$  of 30 mL/kg was attenuated in the Akt-deficient mice, and pharmacologic inhibition was observed with TSA treatment (Fig 6A and 6B). Consistent with the immunohistochemical results, Western blot analyses revealed increased Akt phosphorylation in the mice subjected to a  $V_T$  of 30 mL/kg compared with those subjected to a  $V_T$  of 6 mL/kg and the non-ventilated control mice. However, total Akt nonphosphorylated protein expression did not change significantly. Moreover, the MV-induced phospho-Akt activation was markedly reduced by Akt heterozygous knockout and TSA administration (Fig 6C). However, the increased HDAC4 expression after MV was not attenuated in the Akt-deficient mice, suggesting that HDAC4 is the upstream regulator of Akt signaling involved in ventilation-induced lung fibrogenesis (Fig 6D).

### Inhibition of MV-induced lung inflammation and EMT by Akt heterozygous knockout

Finally, we examined whether the beneficial effects of TSA administration were mediated through the Akt pathway in Akt-deficient mice. Overall, the effects of high- $V_T$  lung stretching on increases in lung EBD leak; BAL fluid total protein; oxidative stress; MMP-9 and PAI-1 protein production; mRNA expressions of collagen 1a1, fibronectin, and MMP-9; fibrogenic markers; and fibrosis scoring in the mice subjected to a  $V_T$  of 30 mL/kg were significantly attenuated in the Akt-deficient mice ( $P < 0.05$ ; Figs 7 and 8). Furthermore, the gas exchange (alveolar–arterial oxygen gradient) in mice receiving a  $V_T$  of 30 mL/kg was considerably improved by TSA treatment and in Akt heterozygous knockout (Table 1).

Because no statistically significant differences were observed between the wild-type and Akt-deficient nonventilated control mice, both with and without bleomycin, the data are not presented in this paper.

Collectively, our results demonstrate that TSA treatment can suppress MV-induced inflammatory responses and lung fibrogenesis, and improve gas exchange in the lung by inhibiting the HDAC4 and Akt pathways (Fig 9).

## Discussion

ARDS is a severe form of lung injury, characterized by increased capillary permeability, pulmonary edema, intense pulmonary inflammation, alveolar epithelial injury, and a high mortality rate [1, 2]. MV is essential to maintain adequate ventilation and gas exchange in patients with ARDS; however, MV by itself can trigger VILI or exacerbate the inflammatory response to fibrosis, resulting in VILI-associated lung fibrosis [3–6]. Accumulating clinical research has highlighted the importance of early identification of fibroproliferation in the lungs of patients with ARDS because a substantial percentage of ARDS survivors ultimately progressed to irreversible pulmonary fibrosis [1, 2]. Thus, early intervention targeting fibroproliferative activity, to ameliorate the progression to subsequent pulmonary fibrosis, may improve clinical outcomes.

In the present study, we demonstrated for the first time that the antifibrotic agent TSA can (1) mitigate the alveolar–capillary membrane leak and oxidative stress; (2) reduce inflammatory cytokines MMP-9 and PAI-1, collagen gene expression, and total collagen production; (3) attenuate the activation of HDAC enzyme specific for HDAC4, but not HDAC2, and suppress Akt phosphorylation; (4) alleviate the EMT process; and (5) ameliorate lung fibrosis as evidenced by improved pathological fibrotic scores, micro-CT images, and restored oxygenation indices in a murine model of MV-augmented bleomycin-induced pulmonary fibrosis. Furthermore, we observed HDAC4 regulated the downstream Akt signaling, and inhibition of HDAC4 and Akt mediates the beneficial effects of TSA in our animal model, which simulated the fibroproliferative response in clinical ARDS.

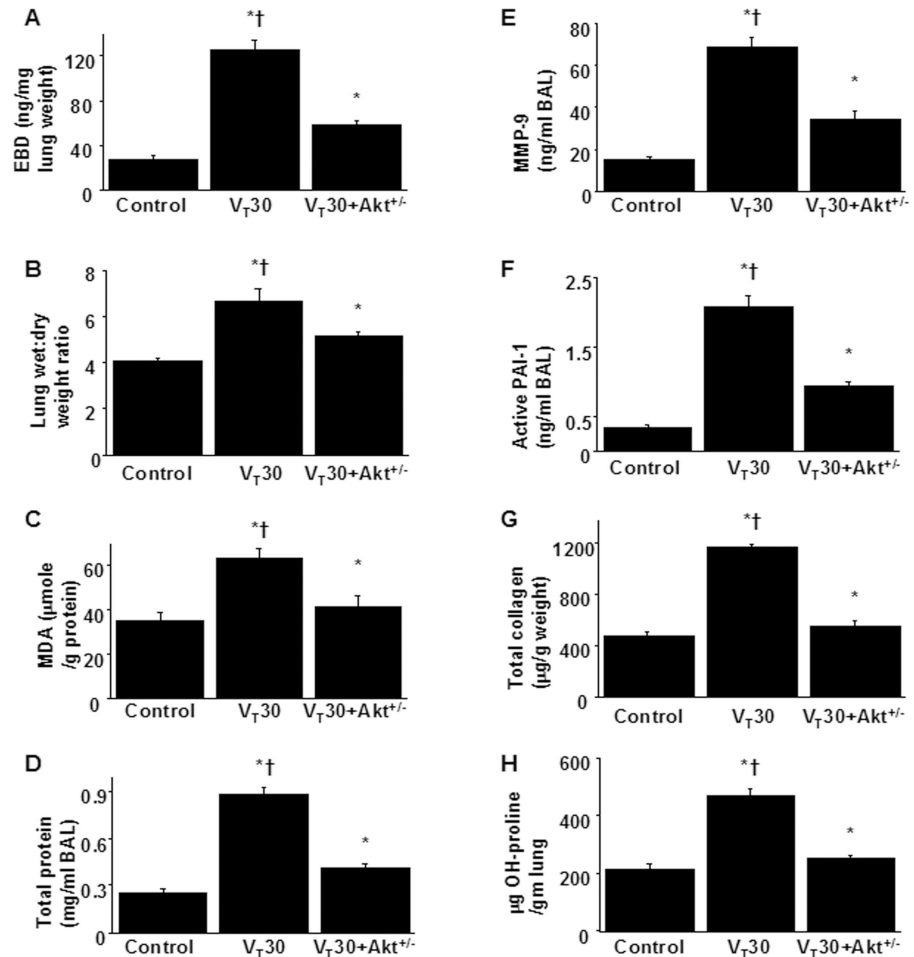


**Fig 7. Inhibition of lung stretch-induced lung inflammation and collagen production by Akt heterozygous knockout.** Five days after administering bleomycin, Evans blue dye secretion (A), lung wet-to-dry-weight ratio (B), BAL fluid total protein (C), MDA (D), MMP-9 (E) and PAI-1 (F) secretion in BAL fluid, total collagen (G), and hydroxyproline (OH) of lung tissue (H) were from the lungs of nonventilated control mice and mice ventilated at a tidal volume 30 mL/kg for 5 h with room air (n = 5 per group). ANOVA was used to assess the statistical significance of the differences, followed by multiple comparisons with a Scheffe's test, and a P value < 0.05 was considered statistically significant. \* P < 0.05 versus the nonventilated control mice with bleomycin pretreatment; †P < 0.05 versus Akt<sup>+/-</sup> group.

doi:10.1371/journal.pone.0172571.g007

The fibroproliferative phase following acute exudative pulmonary inflammation has been previously considered a feature of late ARDS, characterized by fibroblast accumulation and ECM deposition in the injured lungs. However, clinical evidence has highlighted that increased fibroproliferative activity begins within 24 h of ARDS onset [2, 41]. Moreover, the development of pulmonary fibrosis has been associated with increased mortality, ventilator dependence, and restrictive lung disease, resulting in poor prognosis for both short- and long-term clinical outcomes [1, 2, 10]. The devastating role of MV in VILI-associated lung fibrosis has been confirmed in both in vitro and in vivo studies [3–8]. Specifically, high mechanical stresses disrupt the alveolar epithelial lining and lead to EMT activation in primary mammalian alveolar type II epithelial cells and cultured human lung epithelial cells [5, 6]. Additionally, the application of MV in animal models of ALI can induce epithelial injury and facilitate the development of pulmonary fibrosis by activating TGF-β1-induced EMT [5]. These study results suggest that MV can trigger EMT in diseased lungs and facilitate the progression of

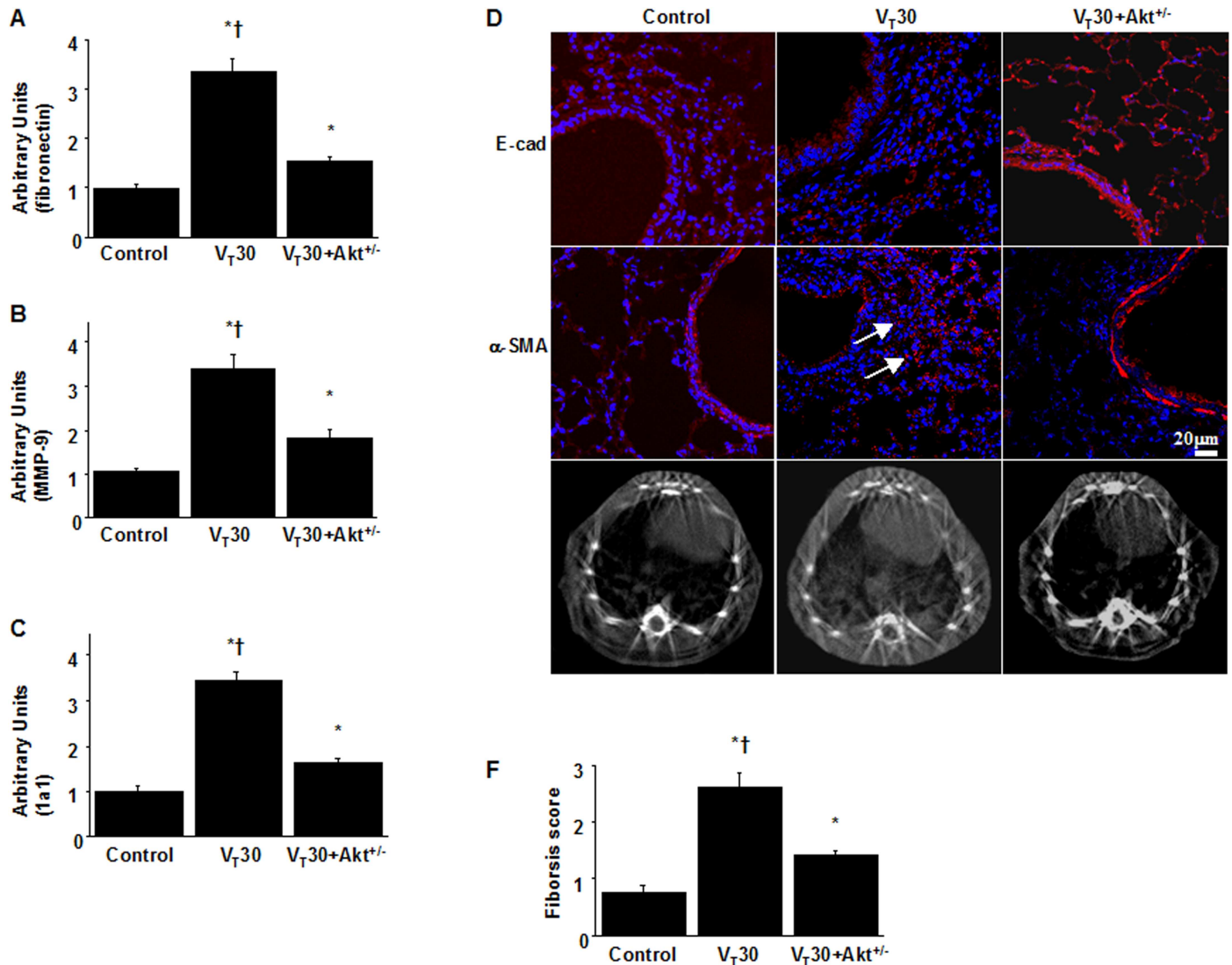


**Fig 8. Reduction of lung stretch-induced collagen gene expression and epithelial-mesenchymal transition in Akt-deficient mice.** After five days of bleomycin treatment, real-time polymerase chain reaction of fibronectin (A), MMP-9 (B), and 1a1 (C) mRNA expression were from the lungs of nonventilated control mice and mice ventilated at a tidal volume of 30 mL/kg for 5 h with room air (n = 5 per group). Arbitrary units were expressed as the ratio of fibronectin, MMP-9, and 1a1 mRNA to GAPDH (n = 5 per group). Representative photomicrographs (x400) with E-cad (red),  $\alpha$ -SMA (red), and Hoechst (blue) immunofluorescent staining of paraffin lung sections (D) (n = 5 per group), and micro-computed tomography imaging (E) (n = 3 per group) five days after administering bleomycin were from nonventilated control mice and mice ventilated at a tidal volume of 30 mL/kg for 5 h with room air. Positive red staining in the fibroblasts is identified by arrows (n = 5 per group). The fibrotic scoring (F) was quantified as the average number of 10 nonoverlapping fields in Masson's trichrome staining of paraffin lung sections (n = 5 per group). Scale bars represent 20  $\mu$ m. ANOVA was used to assess the statistical significance of the differences, followed by multiple comparisons with a Scheffe's test, and a P value < 0.05 was considered statistically significant. \* P < 0.05 versus the nonventilated control mice with bleomycin pretreatment; †P < 0.05 versus Akt<sup>+/-</sup> group.

doi:10.1371/journal.pone.0172571.g008

lung fibrosis. Hence, MV-induced EMT is considered to play a critical role in initiating and propagating VILI-associated lung fibrosis. In agreement with our previous findings, we demonstrated that high-V<sub>T</sub> MV induced and augmented the destruction of the alveolar epithelial barrier and increased capillary permeability, oxidative stress, EMT, profibrotic cytokines regulating ECM remodeling, and excess fibronectin assembly in our VILI and MV-augmented bleomycin-induced pulmonary fibrosis animal models [7, 8, 36]. However, there are no specific pharmacological agents aimed at preventing early fibroproliferation in the lungs of

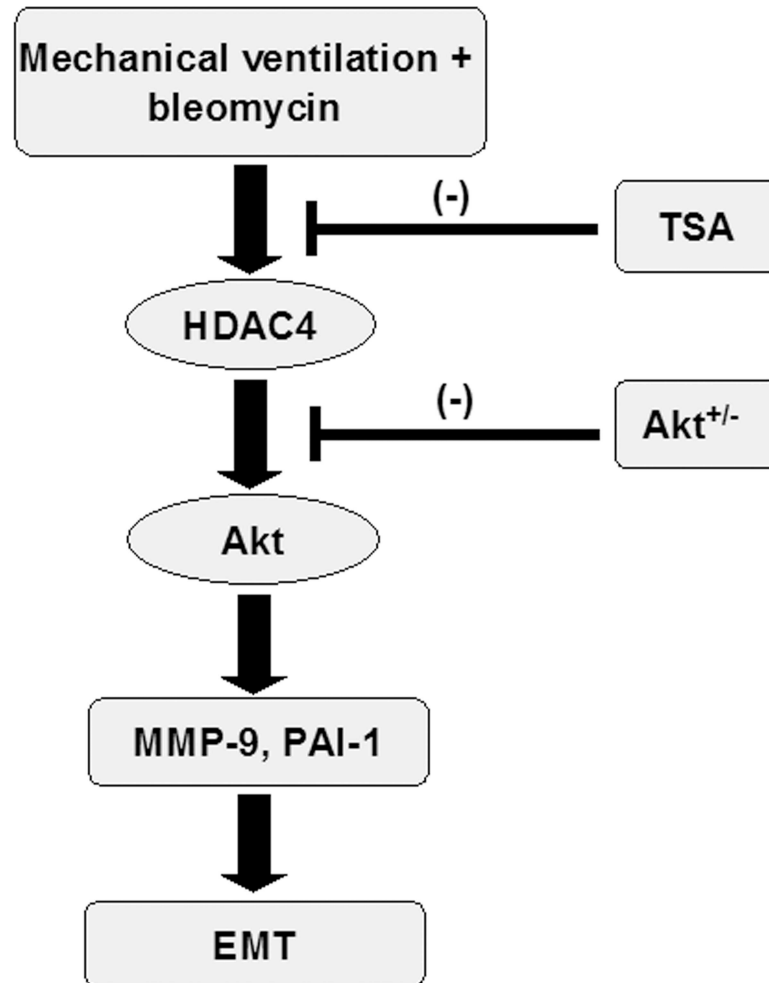


**Fig 9. Schematic figure illustrating the signaling pathway activation with mechanical ventilation.** Bleomycin-induced augmentation of mechanical stretch-mediated cytokine production and EMT were attenuated by the administration of trichostatin A and with Akt heterozygous knockout. Akt<sup>+/-</sup> = Akt-deficient mice; EMT = epithelial-mesenchymal transition; HDAC = histone deacetylase; MMP-9 = matrix metalloproteinase-9; PAI-1 = plasminogen activator inhibitor-1; TSA = trichostatin A.

doi:10.1371/journal.pone.0172571.g009

patients with ARDS. The use of corticosteroids, a nonspecific anti-inflammatory agent, might shorten the MV duration; however, the steroids have the side effect of immunity suppression, and their clinical impact on improving ARDS survival remains unproven [42–44]. These uncertainties raise clinical urgency for investigating the molecular mechanisms involved in early fibroproliferation of ARDS and developing an effective therapy to inhibit EMT and lung fibrosis.

Human HDACs are divided into four classes according to their homology to yeast. Class I HDACs (HDAC 1, 2, 3, and 8) are primarily nuclear enzymes. Class II HDACs (HDAC 4, 5, 6, 7, 9, and 10) are expressed in a tissue-specific manner and shuttle between the nucleus and cytoplasm. Moreover, both class I and class II HDACs are zinc metalloenzymes that catalyze the hydrolysis of acetylated lysine residue. Class II HDACs have also been demonstrably crucial in the control of myofibroblast and smooth muscle functioning. Class III HDACs contain NAD<sup>+</sup>-dependent deacetylases (sirtuin 1–7), and class IV HDAC comprises HDAC11 only [13]. During acute inflammation, histone acetylation and deacetylation changes are involved

in the induction of inflammatory cytokines, and subsequently, the mediation of EMT, fibroblast activation, and proliferation if inflammation persists and progresses to succeeding fibrogenesis [12, 20]. Tissue-specific HDACs are highly expressed and activated in inflamed tissues, epigenetically regulating the local production of PAI-1 and MMP-9 [45, 46]. Furthermore, PAI-1 and MMP-9 are relevant to neutrophil infiltration, EMT, fibroblast proliferation, and ECM remodeling in ALI [9, 21]. Overexpression and upregulation of HDACs, and increased levels of MMP-9 and PAI-1 in the lungs, have been identified in IPF clinical studies [9, 15, 46]. Among the various HDACs, HDAC2 and HDAC4 have been reported to be crucial in modulating cytokine signaling for immune responses [11, 25].

In the present study, we found that high- $V_T$  MV augmented total HDAC activity, as well as PAI-1 and MMP-9 generation following bleomycin exposure. In particular, the pulmonary expression of nuclear HDAC4 significantly increased following MV-augmented lung fibrosis compared with HDAC2; this indicates that class II HDAC4 intensely translocated from the cytoplasm into the nucleus in the injured lungs, whereas class I HDAC2 was not altered. Thus, abrogation of HDAC4 activity by the HDAC inhibitor resulted in the exacerbated suppression of PAI-1 and MMP-9. Our results are in agreement with the findings of a previous *in vitro* study demonstrating that HDAC4 mediated the fibroblast to myofibroblast transition induced by TGF- $\beta$ , and that HDAC4 knockdown inhibited TGF- $\beta$  signaling in human lung fibroblasts [19]. On the basis of these results, the profibrotic effects of HDAC enzymes provide a promising therapeutic option in the management of VILI-associated pulmonary fibrosis using HDAC inhibitors.

TSA selectively inhibits the class I and class II mammalian HDACs and has been reported to have anti-inflammatory and antifibrotic activities both *in vitro* and *in vivo* [19, 33]. TSA can also inhibit the proliferation, migration, and differentiation to myofibroblasts and TGF- $\beta$ -induced collagen secretion in primary human lung fibroblasts [19]. In animal models of bleomycin-induced pulmonary fibrosis, TSA treatment can prevent or inhibit pulmonary fibrosis identified by improving pathological fibrotic scores [33, 47]. In addition to its antineoplastic effects, TSA has been reported to produce antifibrotic effects through the inhibition of EMT in *in vitro* studies of human airway epithelia [23, 28]. Taken together, these findings triggered our interest to investigate the protective effects and molecular mechanisms of TSA on VILI-associated lung fibrosis in our animal model. Guo et al. demonstrated that TSA can blunt  $\alpha$ -SMA and  $\alpha$ 1 type I collagen expression and ameliorate TGF- $\beta$ -mediated myofibroblast differentiation by inhibiting HDAC4 in normal human lung fibroblasts [19]. Although these results are limited to *in vitro* conditions, they implicate the profibrotic role of HDAC4 in mediating the antifibrotic effects exerted by TSA.

In the present study, we demonstrated that TSA prevented EMT and increases in MMP-9 and PAI-1, collagen 1a1, total collagen, and lung fibrosis parameters through the inhibition of HDAC4 activation *in vivo*. Notably, TSA can also function as an autophagy-blocking agent in addition to its inhibitory effect on HDACs. Zhang et al. reported that TSA pretreatment improves MV-induced pulmonary permeability, lung edema, and neutrophilic inflammation, while also inhibiting stretch-induced autophagy activation in injured lungs [48]. These results are in agreement with our findings, and suggest that TSA provides beneficial effects on MV-associated lung damage and fibrosis because of the molecular mechanisms associated with modulating HDACs or autophagy-related genes.

The Akt pathway is required for TGF- $\beta$ 1-induced differentiation of mouse embryonic mesenchymal cells into smooth muscle cells characterized by  $\alpha$ -SMA expression [34]. Specifically, Akt phosphorylation is elevated in fibroblasts isolated from the lungs of bleomycin-injured mice, and Akt inhibition attenuates the lung fibrinogenic activity [40]. One previous *in vitro* study demonstrated that Akt activation was enhanced by HDAC4 through the inhibition of protein phosphatase-mediated Akt dephosphorylation in the regulation of TGF- $\beta$ 1-mediated  $\alpha$ -SMA

expression in human lung fibroblasts [19]. Notably, Tan et al. reported that Akt was involved in the pathway regulating EMT in a mouse model of bleomycin-induced lung injury [35]. Additionally, in our previous study, we demonstrated that high- $V_T$  MV augmented pulmonary fibrosis through the activation of Akt signaling using an *in vivo* bleomycin mouse model [36].

In the present study, we hypothesized that HDAC enzymes regulate the Akt pathway and lead to EMT and fibrosis. First, we proved that genetic downregulation of Akt can effectively reduce MV-augmented bleomycin-induced EMT and pulmonary fibrosis, as indicated by the diminished markers of vascular leakage and oxidative stress, decreased MMP-9 and PAI-1 production and Akt phosphorylation, decrement of total lung collagen, improved EMT profiles and pathological fibrotic alterations, and micro-CT images. Furthermore, Akt was demonstrated to be downstream to HDAC signaling (according to the finding that HDAC inhibition by TSA inhibited Akt activation), but HDAC4 expression was not suppressed in the Akt-deficient mice. Notably, we demonstrated that TSA can attenuate the EMT process, as evidenced by the increased localized epithelial marker (E-cadherin) and decreased localized mesenchymal marker ( $\alpha$ -SMA) in our mouse model of MV-augmented bleomycin-induced pulmonary fibrosis, and that the beneficial effect is mediated through HDAC4-Akt signaling.

According to our review of the relevant literature, only one *in vitro* study by Guo et al. demonstrated that TSA can reduce TGF- $\beta$ 1-induced  $\alpha$ -SMA expression associated with decreased Akt phosphorylation in normal human lung fibroblasts [19]. No *in vivo* study has investigated the effects and mechanisms of TSA on VILI-associated EMT and pulmonary fibrosis previously. Therefore, the present study is the first to demonstrate *in vivo* that TSA can mitigate EMT and subsequent pulmonary fibrosis in mice subjected to bleomycin exposure following MV, which simulates fibroproliferation in ARDS. In addition, we demonstrated that extensive epithelial injury results in increased alveolar capillary permeability and inflammatory parameters in our two-hit animal model. As revealed previously, epithelial cell injury can promote pulmonary fibrogenesis by acquiring a mesenchymal phenotype mediated by HDAC modification [28]. Mechanistically, we also demonstrated that intraperitoneal TSA administration can suppress the activation of HDAC4 and downstream Akt, and attenuate the subsequent pulmonary fibrosis by inhibiting EMT. Our results suggest that inhibition of EMT by TSA is critical to attenuate subsequent fibrogenesis in the setting of acute alveolar-epithelial injury.

Some limitations of our study must be discussed. The use of pan-HDAC inhibitor TSA may have suppressed other HDACs that were not investigated in this study. Previous studies have suggested that HDAC4 integrates with other HDACs, such as HDAC3 or HDAC5, to achieve the modification of chromatin structure and function [49, 50]. Further investigations are necessary to determine what other pathways are involved in the beneficial effects of TSA in VILI-associated pulmonary fibrosis. Additionally, our Akt-deficient mice are Akt heterozygous knockout that induced target mutation in Akt1 gene. The levels of total Akt protein expression were similar between Akt-deficient and wild-type mice because the reduction of Akt1 gene expression was masked by the expression of other isoforms of Akt2 and Akt3 [51–53].

## Conclusions

Our study demonstrated that using the antifibrotic agent HDAC inhibitor TSA can reduce MV-augmented bleomycin-induced pulmonary fibrosis by reducing alveolar capillary leakage, oxidative stress, MMP-9 and PAI-1, and total collagen through the inhibition of EMT, and achieve pathological, radiological, and functional improvements in our animal model that mimicked the fibroproliferation in ARDS. These beneficial effects are partly mediated through HDAC4-Akt signaling. Our results can be translated into clinical application by using TSA to attenuate early pulmonary fibroproliferation in patients with ARDS requiring MV.

## Supporting information

**S1 Table. Trichostatin A inhibited MV-augmented bleomycin-induced microvascular leak, lung edema, oxygen radicals, MMP-9 and PAI-1 production.** Five days after administering bleomycin, Evans blue dye analysis (A), lung wet-to-dry-weight ratio (B), BAL fluid total protein (C), MDA (D), MMP-9 (E) and PAI-1 (F) secretion in BAL fluid were from the lungs of nonventilated control mice and mice ventilated at a tidal volume of 6 mL/kg ( $V_T$  6) or 30 mL/kg ( $V_T$  30) for 5 h with room air ( $n = 5$  per group). TSA 2 mg/kg was given intraperitoneally 1 h before mechanical ventilation. Data are presented as mean  $\pm$  SD. (XLS)

**S2 Table. Trichostatin A reduced MV-augmented bleomycin-induced activation of HDAC4.** (A) Five days after bleomycin treatment, total HDAC activity was from the lungs of nonventilated control mice and mice ventilated at a tidal volume of 6 mL/kg or 30 mL/kg for 5 h with room air ( $n = 5$  per group). (B and C) Western blots performed using antibodies that recognize HDAC2, HDAC4, and GAPDH expression in lung tissue five days after bleomycin treatment were from nonventilated control mice and mice ventilated at a tidal volume of 6 mL/kg or 30 mL/kg for 5 h with room air ( $n = 5$  per group). (D) Real-time polymerase chain reaction of HDAC4 mRNA and GAPDH mRNA expression in lung tissue after five days of bleomycin treatment were from nonventilated control mice and mice ventilated at a tidal volume of 6 mL/kg or 30 mL/kg for 5 h with room air ( $n = 5$  per group). Arbitrary units were expressed as the ratio of HDAC2 to GAPDH, HDAC4 to GAPDH, and HDAC4 mRNA to GAPDH ( $n = 5$  per group). TSA 2 mg/kg was given intraperitoneally 1 h before mechanical ventilation. Data are presented as mean  $\pm$  SD. (XLS)

**S3 Table. Trichostatin A reduced MV-augmented bleomycin-induced collagen production.** Total collagen (A), and hydroxyproline (OH) (B) of lung tissue after five days of bleomycin administration were from nonventilated control mice and mice ventilated at a tidal volume of 6 mL/kg or 30 mL/kg for 5 h with room air ( $n = 5$  per group). TSA 2 mg/kg was given intraperitoneally 1 h before mechanical ventilation. Data are presented as mean  $\pm$  SD. (XLS)

**S4 Table. Trichostatin A suppressed MV-augmented bleomycin-induced collagen gene expression.** After five days of bleomycin treatment, real-time polymerase chain reaction of fibronectin (A), MMP-9 (B), and 1a1 (C) mRNA expression were from the lungs of nonventilated control mice and mice ventilated at a tidal volume of 6 mL/kg or 30 mL/kg for 5 h with room air ( $n = 5$  per group). Arbitrary units were expressed as the ratio of fibronectin, MMP-9, and 1a1 mRNA to GAPDH ( $n = 5$  per group). TSA 2 mg/kg was given intraperitoneally 1 h before mechanical ventilation. Data are presented as mean  $\pm$  SD. (XLS)

**S5 Table. Trichostatin A attenuated MV-augmented bleomycin-induced fibrogenic biomarkers.** Five days after bleomycin treatment, the fibrotic scoring (A) was quantified as the average number of 10 nonoverlapping fields in Masson's trichrome staining of paraffin lung sections ( $n = 5$  per group) were from nonventilated control mice and mice ventilated at a tidal volume of 6 mL/kg or 30 mL/kg for 5 h with room air. TSA 2 mg/kg was given intraperitoneally 1 h before mechanical ventilation. Data are presented as mean  $\pm$  SD. (XLS)

**S6 Table. Trichostatin A and Akt heterozygous knockout abrogated MV-augmented bleomycin-induced Akt phosphorylation.** (A) Representative micrographs (x400) with

phosphorylated Akt staining of paraffin lung sections and quantification 5 days after administering bleomycin were from nonventilated control mice and mice ventilated at a tidal volume of 6 mL/kg or 30 mL/kg for 5 h with room air (n = 5 per group). (B and C) Western blots were performed using an antibody that recognize the phosphorylated Akt expression and antibodies that recognize total Akt, HDAC4, and GAPDH expression in lung tissue five days after bleomycin treatment from nonventilated control mice and mice ventilated at a tidal volume of 6 mL/kg or 30 mL/kg for 5 h with room air (n = 5 per group). Arbitrary units were expressed as the ratio of phospho-Akt to Akt and HDAC4 to GAPDH (n = 5 per group). TSA 2 mg/kg was given intraperitoneally 1 h before mechanical ventilation. Data are presented as mean  $\pm$  SD. (XLS)

**S7 Table. Inhibition of MV-augmented bleomycin-induced lung inflammation and collagen production by Akt heterozygous knockout.** Five days after administering bleomycin, Evans blue dye analysis (A), lung wet-to-dry-weight ratio (B), BAL fluid total protein (C), MDA (D), MMP-9 (E) and PAI-1 (F) secretion in BAL fluid, total collagen (G), and hydroxyproline (OH) of lung tissue (H) were from the lungs of nonventilated control mice, and wild type and Akt-deficient mice ventilated at a tidal volume 30 mL/kg for 5 h with room air (n = 5 per group). Data are presented as mean  $\pm$  SD. (XLS)

**S8 Table. Reduction of MV-augmented bleomycin-induced collagen gene expression and epithelial-mesenchymal transition in Akt-deficient mice.** After five days of bleomycin treatment, real-time polymerase chain reaction of fibronectin (A), MMP-9 (B), and 1a1 (C) mRNA expression were from the lungs of nonventilated control mice, and wild-type and Akt-deficient mice ventilated at a tidal volume of 30 mL/kg for 5 h with room air (n = 5 per group). Arbitrary units were expressed as the ratio of fibronectin, MMP-9, and 1a1 mRNA to GAPDH (n = 5 per group). The fibrotic scoring (D) was quantified as the average number of 10 nonoverlapping fields in Masson's trichrome staining of paraffin lung sections (n = 5 per group) five days after administering bleomycin were from nonventilated control mice, and wild type and Akt-deficient mice ventilated at a tidal volume of 30 mL/kg for 5 h with room air. Data are presented as mean  $\pm$  SD. (XLS)

## Acknowledgments

We thank Chang-Hung Tien, Laboratory Animal Center, Molecular Imaging Center, and Microscope Core Laboratory, Chang Gung Memorial Hospital, Linkou for their help with the experiment.

## Author Contributions

**Conceptualization:** LFL YYL.

**Data curation:** LFL.

**Formal analysis:** LFL YYL.

**Funding acquisition:** LFL CSL.

**Investigation:** LFL.

**Project administration:** LFL YYL.

**Resources:** CSL LFL.

**Software:** LFL YYL.

**Supervision:** NHC CSL CWL LPC CYH.

**Validation:** LFL YYL.

**Visualization:** NHC CSL CWL LPC CYH.

**Writing – original draft:** LFL YYL.

**Writing – review & editing:** LFL YYL.

## References

1. Burnham EL, Janssen WJ, Riches DW, Moss M, Downey GP. The fibroproliferative response in acute respiratory distress syndrome: mechanisms and clinical significance. *Eur Respir J*. 2014; 43(1):276–85. doi: [10.1183/09031936.00196412](https://doi.org/10.1183/09031936.00196412) PMID: [23520315](https://pubmed.ncbi.nlm.nih.gov/23520315/)
2. Marshall RP, Bellingan G, Webb S, Puddicombe A, Goldsack N, McAnulty RJ, et al. Fibroproliferation occurs early in the acute respiratory distress syndrome and impacts on outcome. *Am J Respir Crit Care Med*. 2000; 162(5):1783–8. doi: [10.1164/ajrccm.162.5.2001061](https://doi.org/10.1164/ajrccm.162.5.2001061) PMID: [11069813](https://pubmed.ncbi.nlm.nih.gov/11069813/)
3. Zhang R, Pan Y, Fanelli V, Wu S, Luo AA, Islam D, et al. Mechanical Stress and the Induction of Lung Fibrosis via the Midkine Signaling Pathway. *Am J Respir Crit Care Med*. 2015; 192(3):315–23. doi: [10.1164/rccm.201412-2326OC](https://doi.org/10.1164/rccm.201412-2326OC) PMID: [25945397](https://pubmed.ncbi.nlm.nih.gov/25945397/)
4. Villar J, Cabrera NE, Valladares F, Casula M, Flores C, Blanch L, et al. Activation of the Wnt/beta-Catenin Signaling Pathway by Mechanical Ventilation Is Associated with Ventilator-Induced Pulmonary Fibrosis in Healthy Lungs. *PLoS One*. 2011; 6(9):e23914. doi: [10.1371/journal.pone.0023914](https://doi.org/10.1371/journal.pone.0023914) PMID: [21935365](https://pubmed.ncbi.nlm.nih.gov/21935365/)
5. Cabrera-Benitez NE, Parotto M, Post M, Han B, Spieth PM, Cheng WE, et al. Mechanical stress induces lung fibrosis by epithelial-mesenchymal transition. *Crit Care Med*. 2012; 40(2):510–7. doi: [10.1097/CCM.0b013e31822f09d7](https://doi.org/10.1097/CCM.0b013e31822f09d7) PMID: [21926573](https://pubmed.ncbi.nlm.nih.gov/21926573/)
6. Heise RL, Stober V, Cheluvvaraju C, Hollingsworth JW, Garantziotis S. Mechanical Stretch Induces Epithelial-Mesenchymal Transition in Alveolar Epithelia via Hyaluronan Activation of Innate Immunity. *J Biol Chem*. 2011; 286(20):17435–44. doi: [10.1074/jbc.M110.137273](https://doi.org/10.1074/jbc.M110.137273) PMID: [21398522](https://pubmed.ncbi.nlm.nih.gov/21398522/)
7. Li LF, Chu PH, Hung CY, Kao WW, Lin MC, Liu YY, et al. Lumican regulates ventilation-induced epithelial-mesenchymal transition through extracellular signal-regulated kinase pathway. *Chest*. 2013; 143(5):1252–60. doi: [10.1378/chest.12-2058](https://doi.org/10.1378/chest.12-2058) PMID: [23154825](https://pubmed.ncbi.nlm.nih.gov/23154825/)
8. Li LF, Liu YY, Kao KC, Wu CT, Chang CH, Hung CY, et al. Mechanical ventilation augments bleomycin-induced epithelial-mesenchymal transition through the Src pathway. *Lab Invest*. 2014; 94(9):1017–29. doi: [10.1038/labinvest.2014.75](https://doi.org/10.1038/labinvest.2014.75) PMID: [24955896](https://pubmed.ncbi.nlm.nih.gov/24955896/)
9. Liu RM. Oxidative stress, plasminogen activator inhibitor 1, and lung fibrosis. *Antioxid Redox Signal*. 2008; 10(2):303–19. doi: [10.1089/ars.2007.1903](https://doi.org/10.1089/ars.2007.1903) PMID: [17979497](https://pubmed.ncbi.nlm.nih.gov/17979497/)
10. Cabrera-Benitez NE, Laffey JG, Parotto M, Spieth PM, Villar J, Zhang HB, et al. Mechanical Ventilation-associated Lung Fibrosis in Acute Respiratory Distress Syndrome A Significant Contributor to Poor Outcome. *Anesthesiology*. 2014; 121(1):189–98. doi: [10.1097/ALN.0000000000000264](https://doi.org/10.1097/ALN.0000000000000264) PMID: [24732023](https://pubmed.ncbi.nlm.nih.gov/24732023/)
11. Blanchard F, Chipoy C. Histone deacetylase inhibitors: new drugs for the treatment of inflammatory diseases? *Drug Discov Today*. 2005; 10(3):197–204. doi: [10.1016/S1359-6446\(04\)03309-4](https://doi.org/10.1016/S1359-6446(04)03309-4) PMID: [15708534](https://pubmed.ncbi.nlm.nih.gov/15708534/)
12. Pang M, Zhuang S. Histone deacetylase: a potential therapeutic target for fibrotic disorders. *J Pharmacol Exp Ther*. 2010; 335(2):266–72. doi: [10.1124/jpet.110.168385](https://doi.org/10.1124/jpet.110.168385) PMID: [20719940](https://pubmed.ncbi.nlm.nih.gov/20719940/)
13. Gregoretti IV, Lee YM, Goodson HV. Molecular evolution of the histone deacetylase family: functional implications of phylogenetic analysis. *J Mol Biol*. 2004; 338(1):17–31. doi: [10.1016/j.jmb.2004.02.006](https://doi.org/10.1016/j.jmb.2004.02.006) PMID: [15050820](https://pubmed.ncbi.nlm.nih.gov/15050820/)
14. Kaimori A, Potter JJ, Choti M, Ding Z, Mezey E, Koteish AA. Histone deacetylase inhibition suppresses the transforming growth factor beta1-induced epithelial-to-mesenchymal transition in hepatocytes. *Hepatology*. 2010; 52(3):1033–45. doi: [10.1002/hep.23765](https://doi.org/10.1002/hep.23765) PMID: [20564330](https://pubmed.ncbi.nlm.nih.gov/20564330/)
15. Korfei M, Skwarna S, Henneke I, MacKenzie B, Klymenko O, Saito S, et al. Aberrant expression and activity of histone deacetylases in sporadic idiopathic pulmonary fibrosis. *Thorax*. 2015; 70(11):1022–32. doi: [10.1136/thoraxjnl-2014-206411](https://doi.org/10.1136/thoraxjnl-2014-206411) PMID: [26359372](https://pubmed.ncbi.nlm.nih.gov/26359372/)
16. Mani SK, Kern CB, Kimbrough D, Addy B, Kasiganesan H, Rivers WT, et al. Inhibition of class I histone deacetylase activity represses matrix metalloproteinase-2 and -9 expression and preserves LV function

- postmyocardial infarction. *Am J Physiol Heart Circ Physiol*. 2015; 308(11):H1391–401. doi: [10.1152/ajpheart.00390.2014](https://doi.org/10.1152/ajpheart.00390.2014) PMID: [25795711](https://pubmed.ncbi.nlm.nih.gov/25795711/)
17. Yoshikawa M, Hishikawa K, Marumo T, Fujita T. Inhibition of histone deacetylase activity suppresses epithelial-to-mesenchymal transition induced by TGF-beta1 in human renal epithelial cells. *J Am Soc Nephrol*. 2007; 18(1):58–65. doi: [10.1681/ASN.2005111187](https://doi.org/10.1681/ASN.2005111187) PMID: [17135397](https://pubmed.ncbi.nlm.nih.gov/17135397/)
  18. Glenisson W, Castronovo V, Waltregny D. Histone deacetylase 4 is required for TGFbeta1-induced myofibroblastic differentiation. *Biochim Biophys Acta*. 2007; 1773(10):1572–82. doi: [10.1016/j.bbamcr.2007.05.016](https://doi.org/10.1016/j.bbamcr.2007.05.016) PMID: [17610967](https://pubmed.ncbi.nlm.nih.gov/17610967/)
  19. Guo W, Shan B, Klingsberg RC, Qin X, Lasky JA. Abrogation of TGF-beta1-induced fibroblast-myofibroblast differentiation by histone deacetylase inhibition. *Am J Physiol Lung Cell Mol Physiol*. 2009; 297(5):L864–70. doi: [10.1152/ajplung.00128.2009](https://doi.org/10.1152/ajplung.00128.2009) PMID: [19700647](https://pubmed.ncbi.nlm.nih.gov/19700647/)
  20. Rahman I, Marwick J, Kirkham P. Redox modulation of chromatin remodeling: impact on histone acetylation and deacetylation, NF-kappaB and pro-inflammatory gene expression. *Biochem Pharmacol*. 2004; 68(6):1255–67. doi: [10.1016/j.bcp.2004.05.042](https://doi.org/10.1016/j.bcp.2004.05.042) PMID: [15313424](https://pubmed.ncbi.nlm.nih.gov/15313424/)
  21. Pelosi P, Rocco PR. Effects of mechanical ventilation on the extracellular matrix. *Intensive Care Med*. 2008; 34(4):631–9. doi: [10.1007/s00134-007-0964-9](https://doi.org/10.1007/s00134-007-0964-9) PMID: [18264691](https://pubmed.ncbi.nlm.nih.gov/18264691/)
  22. Cetinkaya M, Cansev M, Cekmez F, Tayman C, Canpolat FE, Kafa IM, et al. Protective Effects of Valproic Acid, a Histone Deacetylase Inhibitor, against Hyperoxic Lung Injury in a Neonatal Rat Model. *PLoS One*. 2015; 10(5):e0126028. doi: [10.1371/journal.pone.0126028](https://doi.org/10.1371/journal.pone.0126028) PMID: [25938838](https://pubmed.ncbi.nlm.nih.gov/25938838/)
  23. Davies ER, Haïtchi HM, Thatcher TH, Sime PJ, Kottmann RM, Ganesan A, et al. Spiruchostatin A inhibits proliferation and differentiation of fibroblasts from patients with pulmonary fibrosis. *Am J Respir Cell Mol Biol*. 2012; 46(5):687–94. doi: [10.1165/rcmb.2011-0040OC](https://doi.org/10.1165/rcmb.2011-0040OC) PMID: [22246864](https://pubmed.ncbi.nlm.nih.gov/22246864/)
  24. Sanders YY, Hagood JS, Liu H, Zhang W, Ambalavanan N, Thannickal VJ. Histone deacetylase inhibition promotes fibroblast apoptosis and ameliorates pulmonary fibrosis in mice. *Eur Respir J*. 2014; 43(5):1448–58. doi: [10.1183/09031936.00095113](https://doi.org/10.1183/09031936.00095113) PMID: [24603818](https://pubmed.ncbi.nlm.nih.gov/24603818/)
  25. Sweet MJ, Shakespear MR, Kamal NA, Fairlie DP. HDAC inhibitors: modulating leukocyte differentiation, survival, proliferation and inflammation. *Immunol Cell Biol*. 2012; 90(1):14–22. doi: [10.1038/icb.2011.88](https://doi.org/10.1038/icb.2011.88) PMID: [22024621](https://pubmed.ncbi.nlm.nih.gov/22024621/)
  26. Wang Z, Chen C, Finger SN, Kwajah S, Jung M, Schwarz H, et al. Suberoylanilide hydroxamic acid: a potential epigenetic therapeutic agent for lung fibrosis? *Eur Respir J*. 2009; 34(1):145–55. doi: [10.1183/09031936.00084808](https://doi.org/10.1183/09031936.00084808) PMID: [19224893](https://pubmed.ncbi.nlm.nih.gov/19224893/)
  27. Chen X, Xiao W, Chen W, Luo L, Ye S, Liu Y. The epigenetic modifier trichostatin A, a histone deacetylase inhibitor, suppresses proliferation and epithelial-mesenchymal transition of lens epithelial cells. *Cell Death Dis*. 2013; 4:e884. doi: [10.1038/cddis.2013.416](https://doi.org/10.1038/cddis.2013.416) PMID: [24157878](https://pubmed.ncbi.nlm.nih.gov/24157878/)
  28. Park IH, Kang JH, Shin JM, Lee HM. Trichostatin A Inhibits Epithelial Mesenchymal Transition Induced by TGF-beta1 in Airway Epithelium. *PLoS One*. 2016; 11(8):e0162058. doi: [10.1371/journal.pone.0162058](https://doi.org/10.1371/journal.pone.0162058) PMID: [27571418](https://pubmed.ncbi.nlm.nih.gov/27571418/)
  29. Ghosh AK, Mori Y, Dowling E, Varga J. Trichostatin A blocks TGF-beta-induced collagen gene expression in skin fibroblasts: involvement of Sp1. *Biochem Biophys Res Commun*. 2007; 354(2):420–6. doi: [10.1016/j.bbrc.2006.12.204](https://doi.org/10.1016/j.bbrc.2006.12.204) PMID: [17234156](https://pubmed.ncbi.nlm.nih.gov/17234156/)
  30. Niki T, Rombouts K, De Bleser P, De Smet K, Rogiers V, Schuppan D, et al. A histone deacetylase inhibitor, trichostatin A, suppresses myofibroblastic differentiation of rat hepatic stellate cells in primary culture. *Hepatology*. 1999; 29(3):858–67. doi: [10.1002/hep.510290328](https://doi.org/10.1002/hep.510290328) PMID: [10051490](https://pubmed.ncbi.nlm.nih.gov/10051490/)
  31. Rombouts K, Niki T, Wielant A, Hellemans K, Geerts A. Trichostatin A, lead compound for development of antifibrogenic drugs. *Acta Gastroenterol Belg*. 2001; 64(3):239–46. PMID: [11680040](https://pubmed.ncbi.nlm.nih.gov/11680040/)
  32. Huber LC, Distler JH, Moritz F, Hemmatazad H, Hauser T, Michel BA, et al. Trichostatin A prevents the accumulation of extracellular matrix in a mouse model of bleomycin-induced skin fibrosis. *Arthritis Rheum*. 2007; 56(8):2755–64. doi: [10.1002/art.22759](https://doi.org/10.1002/art.22759) PMID: [17665426](https://pubmed.ncbi.nlm.nih.gov/17665426/)
  33. Ota C, Yamada M, Fujino N, Motohashi H, Tando Y, Takei Y, et al. Histone deacetylase inhibitor restores surfactant protein-C expression in alveolar-epithelial type II cells and attenuates bleomycin-induced pulmonary fibrosis in vivo. *Exp Lung Res*. 2015; 41(8):422–34. doi: [10.3109/01902148.2015.1060275](https://doi.org/10.3109/01902148.2015.1060275) PMID: [26151196](https://pubmed.ncbi.nlm.nih.gov/26151196/)
  34. Lien SC, Usami S, Chien S, Chiu JJ. Phosphatidylinositol 3-kinase/Akt pathway is involved in transforming growth factor-beta1-induced phenotypic modulation of 10T1/2 cells to smooth muscle cells. *Cell Signal*. 2006; 18(8):1270–8. doi: [10.1016/j.cellsig.2005.10.013](https://doi.org/10.1016/j.cellsig.2005.10.013) PMID: [16310342](https://pubmed.ncbi.nlm.nih.gov/16310342/)
  35. Tan ZX, Chen YH, Xu S, Qin HY, Zhang C, Zhao H, et al. Calcitriol inhibits bleomycin-induced early pulmonary inflammatory response and epithelial-mesenchymal transition in mice. *Toxicol Lett*. 2016; 240(1):161–71. doi: [10.1016/j.toxlet.2015.10.022](https://doi.org/10.1016/j.toxlet.2015.10.022) PMID: [26520185](https://pubmed.ncbi.nlm.nih.gov/26520185/)

36. Li LF, Liao SK, Huang CC, Hung MJ, Quinn DA. Serine/threonine kinase-protein kinase B and extracellular signal-regulated kinase regulate ventilator-induced pulmonary fibrosis after bleomycin-induced acute lung injury: a prospective, controlled animal experiment. *Crit Care*. 2008; 12(4):R103. doi: [10.1186/cc6983](https://doi.org/10.1186/cc6983) PMID: [18691424](https://pubmed.ncbi.nlm.nih.gov/18691424/)
37. Takebe M, Oishi H, Taguchi K, Aoki Y, Takashina M, Tomita K, et al. Inhibition of histone deacetylases protects septic mice from lung and splenic apoptosis. *J Surg Res*. 2014; 187(2):559–70. doi: [10.1016/j.jss.2013.10.050](https://doi.org/10.1016/j.jss.2013.10.050) PMID: [24290430](https://pubmed.ncbi.nlm.nih.gov/24290430/)
38. Ding L, Pan R, Huang X, Wang JX, Shen YT, Xu L, et al. Changes in histone acetylation during oocyte meiotic maturation in the diabetic mouse. *Theriogenology*. 2012; 78(4):784–92. doi: [10.1016/j.theriogenology.2012.03.026](https://doi.org/10.1016/j.theriogenology.2012.03.026) PMID: [22541329](https://pubmed.ncbi.nlm.nih.gov/22541329/)
39. Jin GY, Bok SM, Han YM, Chung MJ, Yoon KH, Kim SR, et al. Effectiveness of rosiglitazone on bleomycin-induced lung fibrosis: Assessed by micro-computed tomography and pathologic scores. *Eur J Radiol*. 2012; 81(8):1901–6. doi: [10.1016/j.ejrad.2010.12.061](https://doi.org/10.1016/j.ejrad.2010.12.061) PMID: [21296518](https://pubmed.ncbi.nlm.nih.gov/21296518/)
40. Vittal R, Horowitz JC, Moore BB, Zhang H, Martinez FJ, Toews GB, et al. Modulation of pro-survival signaling in fibroblasts by a protein kinase inhibitor protects against fibrotic tissue injury. *Am J Pathol*. 2005; 166(2):367–75. doi: [10.1016/S0002-9440\(10\)62260-2](https://doi.org/10.1016/S0002-9440(10)62260-2) PMID: [15681821](https://pubmed.ncbi.nlm.nih.gov/15681821/)
41. Ichikado K, Muranaka H, Gushima Y, Kotani T, Nader HM, Fujimoto K, et al. Fibroproliferative changes on high-resolution CT in the acute respiratory distress syndrome predict mortality and ventilator dependency: a prospective observational cohort study. *BMJ Open*. 2012; 2(2):e000545. doi: [10.1136/bmjopen-2011-000545](https://doi.org/10.1136/bmjopen-2011-000545) PMID: [22382117](https://pubmed.ncbi.nlm.nih.gov/22382117/)
42. Peter JV, John P, Graham PL, Moran JL, George IA, Bersten A. Corticosteroids in the prevention and treatment of acute respiratory distress syndrome (ARDS) in adults: meta-analysis. *BMJ*. 2008; 336(7651):1006–9. doi: [10.1136/bmj.39537.939039.BE](https://doi.org/10.1136/bmj.39537.939039.BE) PMID: [18434379](https://pubmed.ncbi.nlm.nih.gov/18434379/)
43. Ruan SY, Lin HH, Huang CT, Kuo PH, Wu HD, Yu CJ. Exploring the heterogeneity of effects of corticosteroids on acute respiratory distress syndrome: a systematic review and meta-analysis. *Crit Care*. 2014; 18(2):R63. doi: [10.1186/cc13819](https://doi.org/10.1186/cc13819) PMID: [24708846](https://pubmed.ncbi.nlm.nih.gov/24708846/)
44. Steinberg KP, Hudson LD, Goodman RB, Hough CL, Lanken PN, Hyzy R, et al. Efficacy and safety of corticosteroids for persistent acute respiratory distress syndrome. *N Engl J Med*. 2006; 354(16):1671–84. doi: [10.1056/NEJMoa051693](https://doi.org/10.1056/NEJMoa051693) PMID: [16625008](https://pubmed.ncbi.nlm.nih.gov/16625008/)
45. Barnes PJ, Adcock IM, Ito K. Histone acetylation and deacetylation: importance in inflammatory lung diseases. *Eur Respir J*. 2005; 25(3):552–63. doi: [10.1183/09031936.05.00117504](https://doi.org/10.1183/09031936.05.00117504) PMID: [15738302](https://pubmed.ncbi.nlm.nih.gov/15738302/)
46. Craig VJ, Zhang L, Hagood JS, Owen CA. Matrix metalloproteinases as therapeutic targets for idiopathic pulmonary fibrosis. *Am J Respir Cell Mol Biol*. 2015; 53(5):585–600. doi: [10.1165/rcmb.2015-0020TR](https://doi.org/10.1165/rcmb.2015-0020TR) PMID: [26121236](https://pubmed.ncbi.nlm.nih.gov/26121236/)
47. Ye Q, Li Y, Jiang H, Xiong J, Xu J, Qin H, et al. Prevention of Pulmonary Fibrosis via Trichostatin A (TSA) in Bleomycin Induced Rats. *Sarcoidosis Vasc Diffuse Lung Dis*. 2014; 31(3):219–26. PMID: [25363222](https://pubmed.ncbi.nlm.nih.gov/25363222/)
48. Zhang Y, Liu G, Dull RO, Schwartz DE, Hu G. Autophagy in pulmonary macrophages mediates lung inflammatory injury via NLRP3 inflammasome activation during mechanical ventilation. *American journal of physiology*. 2014; 307(2):L173–85. doi: [10.1152/ajplung.00083.2014](https://doi.org/10.1152/ajplung.00083.2014) PMID: [24838752](https://pubmed.ncbi.nlm.nih.gov/24838752/)
49. Backs J, Backs T, Bezprozvannaya S, McKinsey TA, Olson EN. Histone deacetylase 5 acquires calcium/calmodulin-dependent kinase II responsiveness by oligomerization with histone deacetylase 4. *Mol Cell Biol*. 2008; 28(10):3437–45. doi: [10.1128/MCB.01611-07](https://doi.org/10.1128/MCB.01611-07) PMID: [18332106](https://pubmed.ncbi.nlm.nih.gov/18332106/)
50. Fischle W, Dequiedt F, Hendzel MJ, Guenther MG, Lazar MA, Voelter W, et al. Enzymatic activity associated with class II HDACs is dependent on a multiprotein complex containing HDAC3 and SMRT/N-CoR. *Mol Cell*. 2002; 9(1):45–57. PMID: [11804585](https://pubmed.ncbi.nlm.nih.gov/11804585/)
51. Li LF, Liao SK, Lee CH, Huang CC, Quinn DA. Involvement of Akt and endothelial nitric oxide synthase in ventilation-induced neutrophil infiltration: a prospective, controlled animal experiment. *Crit Care*. 2007; 11(4):R89. doi: [10.1186/cc6101](https://doi.org/10.1186/cc6101) PMID: [17714594](https://pubmed.ncbi.nlm.nih.gov/17714594/)
52. Cho H, Thorvaldsen JL, Chu Q, Feng F, Birnbaum MJ. Akt1/PKBalpha is required for normal growth but dispensable for maintenance of glucose homeostasis in mice. *J Biol Chem*. 2001; 276(42):38349–52. doi: [10.1074/jbc.C100462200](https://doi.org/10.1074/jbc.C100462200) PMID: [11533044](https://pubmed.ncbi.nlm.nih.gov/11533044/)
53. Linnerth-Petrik NM, Santry LA, Petrik JJ, Wootton SK. Opposing functions of Akt isoforms in lung tumor initiation and progression. *PLoS One*. 2014; 9(4):e94595. doi: [10.1371/journal.pone.0094595](https://doi.org/10.1371/journal.pone.0094595) PMID: [24722238](https://pubmed.ncbi.nlm.nih.gov/24722238/)